Stony Brook University

Semiparametric Bayesian modeling of density dependence

A Dissertation Presented

by

Masatoshi Sugeno

to

The Graduate School

in Partial Fulfillment of the

Requirements

for the Degree of

Doctor of Philosophy

in

Marine and Atmospheric Science

Stony Brook University

May 2012

Stony Brook University

The Graduate School

Masatoshi Sugeno

We, the dissertation committee for the above candidate for the

Doctor of Philosophy degree, hereby recommend

acceptance of this dissertation.

Stephan B. Munch – Dissertation Advisor
Adjunct associate professor, School of Marine and Atmospheric Sciences, Stony Brook University

Robert M. Cerrato - Chairperson of Defense
Associate professor, School of Marine and Atmospheric Sciences, Stony Brook University

Scott Ferson
Adjunct professor, School of Marine and Atmospheric Sciences, Stony Brook University

Lev Ginzburg
Professor, Department of Ecology and Evolution, Stony Brook University

George Sugihara
Professor, Scripps Institution of Oceanography, University of California, San Diego

This dissertation is accepted by the Graduate School

Charles Taber
Interim Dean of the Graduate School

Abstract of the Dissertation

Semiparametric Bayesian modeling of density dependence

by

Masatoshi Sugeno

Doctor of Philosophy

in

Marine and Atmospheric Science

Stony Brook University

2012

Density dependence is a foundation of population biology. Analysis of population data with parametric models has long provided estimates of the maximum reproductive rate and the form of density dependence. These in turn determine the limit of sustainable harvest and the population's stability, respectively. However, standard parametric analyses of population data generate incorrect inferences of density dependence in noisy and short series. Therefore, there is a clear need for improved statistical methods for inferring density dependence.

In this thesis, I developed new semiparametric Bayesian (SB) methods for estimating reproductive rates and for identifying forms of density dependence. Using simulated data, I validated the superiority of the SB methods to parametric alternatives. Then, I conducted SB analyses of 285 fish populations' datasets to estimate reproductive rates and to identify the forms of density dependence. I compared the results of the SB analyses with those based on standard parametric analyses of the same datasets. The SB analysis indicated that the forms of density dependence in 3.4% of the datasets are Allee effects, whereas the parametric analysis indicated

1.5%, suggesting that Allee effects are more than twice as often as previously thought. However, both the SB and the parametric model (the linear model) generated essentially the same estimates of the reproductive rates, indicating that the linear model may be a reasonable approach to inferring the reproductive rates of fish populations.

Table of Contents

List of Figures

List of Tables

Acknowledgments

I thank my advisor, Dr. Stephan B. Munch, for taking me as his student and for advising me for six years. Among many things I learned from him, which are too many to list here, I am deeply grateful that I learned a great deal of how scientific and mathematical thinking can lead to solving complex ecological problems. His deep understandings in both theoretical and empirical aspects of ecological studies always inspired me, and the inspiration drove me to learn science and mathematics more than I imagined before starting my Ph.D. at SoMAS. Moreover, without his support and encouragement, I would not have ever completed my Ph.D. thesis. I was very fortunate to have worked with you, Steve.

I thank my committee members, Drs. Robert M. Cerrato, Lev Ginzburg, Scott Ferson, and George Sugihara, for constructive comments on my Ph.D. thesis. To Bob, having a discussion with you always made me feel encouraged and motivated. To Lev and Scott, I am grateful that you took me as an intern at Applied Biomathematics Inc. To Lev, you taught me what it takes to be a great president of a company. To Scott, I am fortunate that you gave me a chance to work on an exciting project on medical decision-making problems. To George, I appreciate that your students and you gave me helpful comments on my very preliminary version of my thesis work in 2011.

I thank current and past members of Munch lab, Kestrel, Santiago, Jorge, Jin, Mark, and Charles, for their invaluable inputs to my thesis projects. From them I learned a wide range of studies in ecology and evolutionary biology. Moreover, having non-scientific conversations with you (also with Jo) was a lot of fun. You guys have been great lab mates.

I appreciate writing help from Santiago (chapter 4 and 5) and Lee Brown from Department of Ecology and Evolution (chapter 5).

To all of the friends that I met since I arrived in Stony Brook in 2005, I thank you for turning Stony Brook into a fun place. In particular, I was fortunate to have great roommates at Schomburg A309, Marcos, Riza (and his wife, Gulay), Gunwoo, Ozan, and Chen. Seeing you at home was always heartwarming.

I want to give special thanks to my friends who shared with me an interest in dancing the tango. In particular, Arzu, Eunah, and Irem, welcomed me to the former official tango club at Stony Brook University. Hernan turned me into a tango fanatic. To those in the current unofficial tango club at Stony Brook University where I am a self-appointed president and an instructor, I thank Betul, Jasmine, Lan, Nissim, Panagiotis, Rae, Soojin, Yuan, Yury, to list some, for constantly coming to weekly practice sessions. By exploring the tango with you, I learned "the pleasure of finding things out".

My Ph.D. thesis projects were supported by a grant awarded to Stephan B. Munch from the National Science Foundation (DEB-0727312).

Chapter 1

Introduction

1-1. General introduction

Density dependence is a foundation of population biology (Turchin 2003). Density-dependent effects arise when the intensity of these effects change with population size. Density dependence can describe a wide range of patterns observed in population dynamics (e.g., steady state dynamics, chaotic dynamics, consumer-resource dynamics, predator-prey interactions, host-parasite dynamics), and has consequently played a pivotal role in the development of population biology (Turchin 2003).

In addition to the long-term interest in density dependence from a theoretical perspective (Turchin 2003), density dependence has considerable practical applications in the management of natural renewable resources, the conservation of endangered species, and the restoration of decimated populations. For example, density dependence can be used for determining the upper limits to harvest (Myers et al. 1997; Myers et al. 1999; Myers 2001) and for establishing optimum harvesting rates for sustainable use (Lande et al. 1994). It can also be used for estimating minimally viable population sizes needed for persistence of a population (Courchamp et al. 2008) and for estimating extinction probability of endangered species (Boukal and Berec 2002; Dennis 2002). Moreover, knowing the nature of density dependence in populations can help in understanding vulnerability to invasion by introduced species, for assessing risk of disease outbreak (Tayler and Hastings 2005; Tobin et al. 2011), and for developing robust restoration programs for collapsed populations (Grevstad 1999; Deredec and Courchamp 2007;

Armstrong and Wittmer 2011). Clearly, the successful implementation of management strategies relies heavily on correctly identifying the form of density dependence.

In practice, a mathematical model is used to obtain an inference of density dependence from population data. The simplest model of density dependence is one where population growth rate is assumed to be a function of current population size:

$$N_{t+1} = N_t \exp[f(N_t)] \quad (1)$$

(Turchin 2003). In this model, N_t is population size at time t and $f(N_t)$ is a function that specifies the form of density dependence. In fisheries, in addition to modeling standard population dynamics as described in Eq. 1, density dependence is used for modeling the relationship between mature adult biomass (spawning stock) and offspring produced (recruitment). The stock-recruitment relationship can be given by:

$$R = S\exp[f(S)] \quad (2)$$

where S is spawning biomass and R is recruitment biomass (Quinn and Deriso 1999). As written, functions $f(N_t)$ and $f(S)$ specify the form of density dependence in these relationships, and the specific choice of parameters determines the behavior of the models. In Table 1, some example functions specifying $f(N_t)$ are provided.

Inferences regarding the nature and strength of density dependence have been typically obtained by analyzing population data using parametric models. In cases when it is uncertain what parametric model should be used to describe density dependence, the best model can be identified by comparing performance of multiple models via a model selection criterion (e.g., likelihood ratio test, AIC, BIC, DIC, posterior predictive loss) (Barrowman and Myers 2000). In addition, the inference of density dependence provided by multiple models can be averaged based on the plausibility of each model if one is worried about the complete ignorance of less

plausible because of the on-and-off nature of the model selection approach (Brodziak and Legault 2005).

Although this parametric approach for identifying the form of density dependence seems appealing, some serious drawbacks are known. First, choice of a model usually limits the possible range of density dependence (e.g., Myers et al. 1994; Zhou 2007). For example, the Ricker model is strictly linear in $f(N_t)$ (Table 1), eliminating the possibility of $f(N_t)$ being better modeled by a nonlinear function. Therefore, when a collection of parametric models used for identifying the form of density dependence does not include the most plausible form of density dependence, an incorrectly specified model can be identified as the best model. Second, although the best model for describing density dependence is expected to be the same regardless of model selection criteria, this is often not the case. Analyses of typically noisy and short ecological time series have shown that the best model can be sensitive to choice of model selection criteria (Hill et al. 2007; Ward 2008). Alternatively, different models can be statistically equally plausible (Wood and Thomas 1999). Worse, a simulation study has demonstrated that model selection criteria can identify an incorrectly specified model as the better model (Shelton and Healey 1999).

Uncertainty in the form of density dependence suggests that previous parametric-based approaches might have generated incorrect inferences of density dependence based on empirical datasets. Using the likelihood ratio test to identify the form of density dependence in datasets of fish populations, Myers et al. (1995) showed that Allee effects (positive density dependence at low population size) were found in <2.4% of the fish populations. Using the Ricker model (negative density dependence), Myers et al. (1999) conducted a meta-analysis of over 700 datasets of fish populations, demonstrating that the maximum reproductive rate of fish

populations is within the 1-7 range in most species. In addition, Myers et al. (1999) concluded that the Ricker model may be the best approximated form of negative density dependence in fish populations. Furthermore, Gregory et al. (2010) analyzed taxonomically broader datasets with parametric models, concluding that Allee effects were found in <1.2% of the datasets. These studies generated the consensus view that negative density dependence is a reasonable approximation for modeling density dependence in wild populations. However, given the drawbacks in analyzing ecological data with parametric models, the inferences of maximum reproductive rate and of density dependence may be largely biased.

1-2. Brief description of chapters in this thesis

The aim of this thesis is to develop a flexible modeling approach to obtain the best form of density dependence. Use of a flexible model was advocated previously (e.g., Bravington et al. 2000), and non/semi-parametric statistical methods were developed for obtaining non/semi-parametric inferences of density dependence (Evans and Rice 1988; Cook 1998; Bravington et al. 2000; Munch et al. 2005). Most of them were shown to perform as good as, or even better than, parametric models in generating inferences of density dependence in stock-recruitment data. However, these methods were not designed to provide specific information for practical use (e.g., maximum reproductive rate and carrying capacity); doing so involves *ad hoc* and error-prone statistical methods. Of all the methods introduced above, I will specifically focus on a semiparametric Bayesian (SB) method that is based on the use of a Gaussian process (GP) prior (Munch et al. 2005), and will extend it to provide information needed among conservation/management practitioners.

In chapter 2, I will develop a conditional GP prior for obtaining a SB estimate of the maximum reproductive rate. I will conduct simulation studies to compare performance of the conditional GP prior with that of other GP priors (e.g., Munch et al. 2005) in terms of estimability of reproductive rate. I will also compare SB estimates of reproductive rate with estimates provided by parametric models. In chapter 3, I will develop a SB approach to identify the form of density dependence in stock-recruitment datasets. Specifically, I will construct a SB index provided by the posterior inference of a GP prior and by the derivative of the GP prior. I will conduct simulation studies to compare performance of the SB approach with its parametric alternatives.

In the last two chapters, I will apply the SB methods developed in chapters 2 and 3 to the analysis of empirical stock-recruitment datasets collected from the 'Stock recruitment database' (http://www.mscs.dal.ca/~myers/welcome.html). In chapter 4, I will estimate reproductive rates of fish populations using the method developed in chapter 2. Then, I will compare the SB estimates of the reproductive rate with estimates provided by parametric models (Myers et al. 1997; Myers et al. 1999). In chapter 5, I will obtain the SB inferences of density dependence using the method developed in chapter 3. Then, I will compare the estimated frequency of Allee effects among fish populations with that provided by parametric alternatives (Myers et al. 1995).

In each chapter, I will discuss the benefits and shortcomings of the SB approach in analyzing ecological data. I will also discuss future directions to further refine the SB analysis.

1-3. Tables:

Table 1. Examples of parametric functions specifying $f(N_t)$ (from Turchin 2003). λ is the population growth rate and k is the carrying capacity. a, b, and θ are some positive constants. The same functional forms are gragusually directly applicable to modeling density dependence in stock-recruitment relationships (Quinn and Deriso 1999; Liermann and Hilborn 2001; Needle 2002).

Density independence	$\ln\lambda$
Quadratic map	$\ln[\lambda(1 - N_t/k)]$
Ricker	$\ln\lambda - aN_t$
Theta-Ricker	$\ln\lambda - aN_t{}^{\theta}$
Beverton-Holt	$\ln\lambda - \ln(1 + aN_t)$
Sigmoid Beverton-Holt	$\ln\lambda + (\theta - 1)\ln N_t - \ln\left(1 + aN_t{}^{\theta}\right)$
Gompertz	$\ln\lambda + (\theta - 1)\ln N_t$

Chapter 2

A semiparametric Bayesian approach to estimating maximum reproductive rates at low population sizes

Key words

Allee effects, depensation, Gaussian process, maximum annual reproductive rate, semiparametric Bayesian modeling, slope at the origin, stock recruitment relationship

Abstract

The maximum annual reproductive rate (i.e., the slope at the origin in a stock-recruitment relationship) is one of the most important biological reference points in fisheries; it can be interpreted as upper limit of sustainable fishing mortality and a growth rate of a stock. Fitting parametric models to stock-recruitment data may not be a robust approach because two statistically indistinguishable models can generate radically different estimates of the maximum annual reproductive rate. To mitigate this issue, we developed a flexible semiparametric Bayesian approach based on conditional Gaussian process priors specifically designed to estimate the maximum annual reproductive rate, and applied it to analyze simulated stock recruitment datasets. Compared with results based on other Gaussian process priors, we found that the conditional Gaussian process prior provided superior results: the accuracy and precision of estimates were enhanced without increasing model complexity. Moreover, compared with parametric alternatives, performance of the conditional Gaussian process prior was comparable to that of the data-generating model and always better than the wrong model.

2-1. Introduction

The maximum annual reproductive rate of a stock is probably one of the most needed information in fisheries sciences. They can be used for two important reference points in fisheries: stocks' upper limit of sustainable fishing mortality and growth rates (Myers et al. 1997; Myers et al. 1999; Myers 2001). In practice, stocks can be exploited sustainably as long as their fishing mortality rates are maintained below their upper limit (Bravington et al. 2000; Cook 2000; Myers et al. 1998). The estimates of stocks' growth rates provide expected time for overharvested stocks for rebuilding (Myers et al. 1997). Although there may be complications involved in applying maximum annual reproductive rates to actual fisheries management (Ludwig 1993; Ostrom et al. 1999; Diez et al. 2003), good estimates are nevertheless an important baseline for sustainable fisheries.

The conventional approach to estimating the maximum annual reproductive rate is to analyze stock-recruitment (SR) data using one or several parametric models (Quinn and Deriso 1999). These models typically have a 'slope at the origin' parameter, denoted by α, which is equivalent to the maximum annual reproductive rate. After fitting several models, the estimate for α is either the estimate associated with the best fitting model (e.g., Barrowman and Myers 2000) or is obtained by model averaging (e.g., Brodziak and Legault 2005).

One potential drawback of this parametric approach is that the choice of the model can limit the possible range of estimates for α (e.g., Myers et al. 1994; Zhou 2007). As a consequence, estimates of α are sensitive to model choice. Worse, model selection criteria (e.g., AIC, BIC, DIC, posterior predictive loss, etc.) are not always robust for finding the best estimates for α, because different models can be statistically indistinguishable when data are few

or noisy, and model performance can be inconsistent across different criteria (Wood and Thomas 1999; Hill et al. 2007; Ward 2008).

Nonparametric statistical methods have been used to circumvent the uncertainty in model structure for a SR relationship (Evans and Rice 1988; Cook 1998; Bravington et al. 2000; Munch et al. 2005), and the need for a nonparametric approach to estimating α was first taken up by Bravington et al. (2000). Bravington et al. (2000) developed constrained nonparametric regression methods explicitly intended to estimate α. However, while the constraints they introduced are reasonable, they are not guaranteed to be true. Moreover, additional information about α is frequently available and can be incorporated in models. In a Bayesian context, for example, information regarding life history of fish can be used to derive an informative prior for α (e.g., He et al. 2006).

Munch et al. (2005) developed a nonparametric Bayesian approach to estimating a SR function using a Gaussian process (GP) prior. Their model retains nonparametric flexibility while allowing the incorporation of prior information and the assumption that recruitment is strictly positive ($R>0$). This approach outperforms incorrectly specified parametric models and is comparable to the correct model in simulation testing. However, there are several obvious ways to improve this model. For instance, a more reasonable prior should also ensure that no recruitment is possible when the stock is absent (i.e., $R=0$ when $S=0$). Moreover, although Munch et al. (2005) provided estimates of $\ln\alpha$, this was accomplished in an *ad hoc* way by numerical differentiation of the inferred SR model which was both computationally intensive and potentially error prone.

In this chapter, we introduce a semiparametric Bayesian (SB) approach specifically designed to estimate $\ln\alpha$ as a parameter while retaining flexibility in the shape of the fitted SR

model. In order to understand the estimability of lnα, we conducted a comprehensive simulation study. Specifically, we assessed how model performance, specifically bias and variance in estimated lnα was affected by the level of noise in the data and the availability of data close to the origin. Performance was compared with that of two commonly used parametric models and the nonparametric Bayesian model of Munch et al. (2005).

2-2. Methods

We begin by reviewing the general approach to estimating the slope at the origin, α, in a SR relationship. We then introduce a conditional Gaussian process (GP) prior that enables us to estimate α as a parameter under a semiparametric Bayesian (SB) framework. Finally, we describe the simulation study used to test the method. Mathematical details are given in Appendix A.

2-2-1. Estimating α from the SR relationship

The relationship between stock size and recruitment can be modeled by:

$$R = S\exp[f(S)] \tag{1}$$

where S is a spawning biomass and R is a recruitment biomass. Density dependence is modeled by $\exp[f(S)]$ using an arbitrary function $f(S)$. The slope at the origin, α, is obtained from Eq 1 by taking the derivative of Eq 1 with respect to S and setting $S = 0$. Doing so yields

$$\alpha = \exp[f(0)] \tag{2}$$

or, equivalently, $\ln\alpha = f(0)$. In the absence of depensation, $f(S)$ is a monotonically decreasing function, and α is guaranteed to be the the maximum reproductive rate. Of course, in the presence of depensation, $f(S)$ contains a global maximum at some $S > 0$, and α is not the

maximum reproductive rate but merely the limiting reproductive rate as population density drops to zero.

In keeping with many prior studies (e.g., Myers et al. 1999; Munch et al. 2005), we assume that S is observed without error and multiply Eq 1 by an error term, $\exp(\varepsilon)$, to account for uncertainty in R given S:

$$R = S\exp[f(S) + \varepsilon] \tag{3}$$

where ε is normally distributed with mean 0 and variance σ^2 but without serial dependence. Under this modeling framework, we explicitly assume that stocks are closed populations (i.e., no migration and emigration) and ensure that R=0 when S=0. For mathematical convenience (see section 2-2-2) and consistency with previous studies (Myers et al. 1999; Myers et al. 2001), we re-write Eq 3 using the transformed variate $y = \ln(R/S)$, leading to

$$y = f(S) + \varepsilon. \tag{4}$$

We use Eq 4 for the remainder of this chapter.

We note that temporal autocorrelation appears to be present in many fisheries data (Myers and Barrowman 1995) and several methods (e.g., Walters 1990; Bence 1995; Pyper and Peterman 1998) are available to correct bias in fitted parametric models. However, we are not aware of comparable bias correction methods for non/semi-parametric models. Development of bias correction terms for semiparametric models is an important area for future research that is beyond the scope of this paper.

2-2-2. A conditional GP prior

Our goal is to develop a semiparametric method that enables us to estimate $\ln\alpha$ as a parameter. To do so, we begin with a GP prior (Munch et al. 2005) which models random

functions $f(S)$ in Eq 4 under a nonparametric Bayesian framework. We then condition this GP prior such that $f(0) = \ln\alpha$ is ensured for all realizations of the random function $f(S)$ resulting in a semiparametric specification.

A GP is a generalization of a multivariate normal distribution whose dimension is infinite (i.e., S is a continuous variable). Typically, a GP prior is specified with a mean function $\mu(S)$ and a covariance function $\Sigma(S, S')$ and we write this prior specification as

$$f(S) \sim \mathrm{GP}[\mu(S), \Sigma(S, S')]. \tag{5}$$

Although many mean functions are possible, here we set the prior mean function to

$$\mu(S) = \ln\alpha + \beta S/\max(S), \tag{6}$$

meaning that the random function $f(S)$ is, on average, linear in the prior over S. Importantly, the posterior mean of this GP prior is not necessarily linear, but will be driven largely by the shape of the data (Munch et al. 2005).

The covariance function $\Sigma(S, S')$ determines how deviations from the mean covary across the input space S. Because commonly used SR functions are continuous and smooth, and we have no *a priori* reason to assume that the uncertainty in $f(S)$ varies with S, we used an isotropic covariance function among other choices (Rasmussen and Williams 2006):

$$\Sigma(S, S') = \tau^2 \exp\left[-\phi \left|\frac{S - S'}{\max(S)}\right|^2\right], \tag{7}$$

where ϕ determines the wiggliness of the random function $f(S)$ and τ^2 determines its vertical range (see Rasmussen and Williams 2006 for details).

Note that $\ln\alpha$ appears explicitly in the model formulation through specification of the prior mean function (Eq 6). However, the realized slope at the origin is $f(0)$ and under this prior specification $f(0) \sim \mathrm{N}[\mu(0), \Sigma(0,0)]$ where the mean is given by $\mu(0) = \ln\alpha$ and the variance is

$\Sigma(0,0) = \tau^2$. Thus the actual slope at the origin $f(0)$ in this naive specification is random. It is not exactly equal to $\ln\alpha$ and realizations of $f(0)$ may deviate widely from true $\ln\alpha$. We eliminate this ambiguity by conditioning the GP prior such that all realizations of $f(S)$ have $f(0)$ exactly equal to $\ln\alpha$, thereby ensuring that $\ln\alpha$ is the slope at the origin in the fitted SR model (see Appendix A). The conditional GP prior is the same as the unconditioned prior (Eqs 5-7) except that the covariance function is replaced by the conditional covariance function $\Sigma_c(S, S')$, i.e.,

$$\Sigma_c(S, S') = \tau^2 \exp\left[-\phi \left|\frac{S - S'}{\max(S)}\right|^2\right] - \tau^2 \exp\left\{-\phi \left[\frac{S^2 + S'^2}{\max(S)^2}\right]\right\}. \quad (8)$$

2-2-3. Prior specification

We used uninformative priors developed previously for parameters $\ln\alpha$ and β in the prior mean and for the noise variance σ^2 (Millar 2002), specifically $\Pr(\ln\alpha, \beta) \propto 1$ and $\Pr(\sigma^2) \propto \sigma^{-2}$. More careful consideration was needed in specifying prior distributions for ϕ and τ^2, because the posterior distributions may not converge when improper priors, such as $\Pr(\phi, \tau^2) \propto \phi^{-1}\tau^{-2}$, are used. As in Munch et al. (2005), we used the range of y (i.e., $r_y = \max(y) - \min(y)$) to provide prior information on the total variance. Since the total prior variation in y is given by $\mathrm{Var}(y) = \mathrm{Var}[f(S)] + \sigma^2$, we assigned the expected prior variance to $f(0)$ by setting $\mathrm{E}(\tau^2) = r_y$. We used a gamma prior, $\Pr(\tau^2) \propto \tau^2 \exp(-2\tau^2/r_y)$. The preliminary prior sensitivity analysis with different parameterization for this prior did not change estimates for $\ln\alpha$ and fits of the GP models to data.

As noted previously, ϕ controls the wiggliness of realizations of $f(S)$. A GP prior with large values for ϕ generates random functions $f(0)$ that have many local extrema over the range

of S. However, biologically plausible SR functions have very few local extrema. For example, the Ricker model has a single maximum and the Beverton-Holt (BH) model has only an asymptote (Quinn and Deriso 1999). In the prior, we therefore allowed *f*(*S*) to have not more than 2 local maxima over *S* so that more complex shapes in *f*(*S*) (such as *f*(*S*) modeling depensatory SR relationship, Quinn and Deriso 1999) were admissible. Although the expected number of local extrema can be found analytically for a zero-mean GP with a stationary covariance function (e.g., Ylvisaker 1965), this is not the case for the present model and we determined the relationship between ϕ and the expected number of turns in *f*(*S*) by simulation.

To do so, we generated random functions *f*(*S*) using the unconditional GP prior (Eqs 5-7) for different combinations of ϕ and τ^2, and counted the number of inflection points in $S\exp[f(S)]$. We found that the result is independent of τ^2 and that $S\exp[f(S)]$ has 2 local extrema on average when $\phi = 8$. Based on this information, we used an informative gamma prior whose mean is $\mathrm{E}(\phi) = 8$, which is specified by $\Pr(\phi) \propto \phi\exp(-\phi/4)$. Note that this prior specification is not overly restrictive; data that are strongly informative about the presence of a greater number of inflection points will overwhelm this prior choice. By specifying the prior in this manner we are seeking to incorporate biological realism and to prevent the model from 'fitting the noise'.

2-2-4. Parameter estimation

For notational convenience, we collect the set of hyperparameters into the vector $\boldsymbol{\Theta} = \{\ln\alpha, \beta, \phi, \tau^2, \sigma^2\}$. With n years of stock biomass and recruitment data, $(\boldsymbol{S}, \boldsymbol{R}) = (\{S_1, \dots, S_n\}, \{R_1, \dots, R_n\})$, we have $\boldsymbol{y} = \{\ln(R_1/S_1), \dots, \ln(R_n/S_n)\}$ and *f*($\boldsymbol{S}$) evaluated at the points in $\boldsymbol{S}$ is a sample from an *n*-dimensional multivariate normal distribution, i.e.,

$$f(\boldsymbol{S})|\ln\alpha,\beta,\phi,\tau^2 \sim \text{MVN}[\mu(\boldsymbol{S}),\Sigma_c(\boldsymbol{S},\boldsymbol{S}')] \quad (9)$$

where the mean vector $\mu(\boldsymbol{S})$ is given by

$$\mu(\boldsymbol{S}) = \ln\alpha\mathbf{1}_{\boldsymbol{n}} + \beta\boldsymbol{S}/\max(\boldsymbol{S}) \quad (10)$$

and the i,j^{th} element of the $n \times n$covariance matrix is

$$\Sigma_c(S,S') = \tau^2\exp\left[-\phi\left|\frac{S_i - S_j}{\max(\boldsymbol{S})}\right|^2\right] - \tau^2\exp\left\{-\phi\left[\frac{{S_i}^2 + {S_j}^2}{\max(\boldsymbol{S})^2}\right]\right\}. \quad (11)$$

Here, $\mathbf{1}_{\boldsymbol{n}}$ is an $n \times 1$ vector of ones. As specified so far, the full Bayesian model is computationally cumbersome to work with. To simplify posterior inference, we integrated over *f*($\boldsymbol{S}$) (see e.g., Munch et al. 2005) and worked with the marginal posterior given by:

$$\boldsymbol{y}|\boldsymbol{S},\boldsymbol{\Theta} \sim \text{MVN}[\mu(\boldsymbol{S}),\Sigma_c(\boldsymbol{S},\boldsymbol{S}') + \sigma^2\mathbf{I}_{\boldsymbol{n}}] \quad (12)$$

$$\boldsymbol{\Theta} \sim \Pr(\boldsymbol{\Theta}), \quad (13)$$

where $\mathbf{I_n}$ is an $n \times n$ identity matrix. As described earlier, the prior distribution of Eq 13 is given by $\Pr(\boldsymbol{\Theta}) \propto 1 \cdot \phi\exp(-\phi/4) \cdot \tau^2\exp\left(-2\tau^2/r_y\right) \cdot \sigma^{-2}$. In this way, we omitted obtaining posterior inference for $f(\boldsymbol{S})$, which is not relevant to estimating $\ln\alpha$,while updating $\boldsymbol{\Theta}$. Note that the model (Eq 12) is an n-dimensional multivariate normal distribution conditioned on $\boldsymbol{\Theta}$ (Eq 13).

We used a Markov Chain Monte Carlo method (Metropolis algorithm, (e.g., Gelman et al. 2003)) to obtain the posterior distribution for $\boldsymbol{\Theta}$. The convergence of the Monte Carlo runs was assessed by comparing the variance within a single run with the variance among multiple runs, where their initial values for the runs were dispersed around initial maximum likelihood estimates (Gelman et al. 2003).

2-2-5. Simulation study

We evaluated the performance of our SB approach using simulated data. Because the Ricker and the BH models are the most common choices for studying a SR relationship (Myers et al. 1999; Quinn and Deriso 1999; Myers et al. 2001; Zhou 2007), we used these two models for generating data sets. Lack of data at low stock sizes and the noise level in data are likely to be the two main sources of uncertainty and bias in estimating $\ln\alpha$ (Hilborn and Walters 1992). In designing our simulation, therefore, we initially generated data from Ricker and BH models with a range of minimal stock sizes, noise levels, and values for $\ln\alpha$. Preliminary analyses indicated that the results are relatively insensitive to variation in $\ln\alpha$ over a reasonable range of values and we therefore used a fixed value of $\ln\alpha=\ln 4$.

We based our simulation design on a preliminary analysis of data from 25 Atlantic cod (*Gadus morhua*) stocks for which 10 or more years of data were available from Ransom Myers' Stock Recruitment Database (http://www.mscs.dal.ca/~myers/welcome.html). In keeping with previous analyses (e.g., Myers et al. 1999), recruitment data for each stock was multiplied by $(1-p)\mathrm{SPR}_{\mathrm{F}=0}$ where $p=\exp(-M)$ and M is natural mortality and $\mathrm{SPR}_{\mathrm{F}=0}$ is the spawning biomass resulting from each recruit in the limit of no fishing mortality. In principle, this transformation provides us with standardized units for α, 'annual' reproductive rates, which allow meaningful comparison across stocks. For each stock, we found the stock size that maximized recruitment and used this to set the scale: the minimum stock size was always less than half of this value while the range of observed stock sizes was less than 1.5 times this value for 19 of the 25 stocks. Further, fitting a Ricker model to these data, we found that 88% of the data sets had estimated values of σ^2 between 0.1 and 1. This analysis is intended to provide us

with a 'realistic' baseline around which to construct our simulation study and is not intended as a rigorous analysis of the cod data.

Using these observations to constrain the design of our simulation, we generated data sets from both the Ricker and the BH models with σ^2 between 0.1 and 1. Since, for simulation purposes, the actual units for stock and recruitment are less important than the level of noise and the *relative* distance to the origin, we set maximum recruitment equal to 1, which sets the stock size that maximizes recruitment equal to e/α=0.68 in our simulated data. With this scaling in mind, we set minimum stock sizes, $S_{\min}$, between 0 and 0.34 and the range of stock sizes equal to 1.02. For each combination of model, σ^2, and $S_{\min}$, we generated 500 replicate data sets which consisted of 30 observations each. Simulated stock sizes were drawn from a uniform distribution on [$S_{\min}$, $S_{\min}$+1.02] and recruitment was calculated using the Ricker or the BH model according to Eq 3.

For each of these data sets, we estimated lnα using the Ricker model, the BH model and the SB approach described above. In what follows, we will refer to this SB approach as the 'linear' model, for reasons that should become clearer shortly. To evaluate the importance of prior specification we also compared the 'linear' model to three alternative GP models that relax the specification of prior information on the shape of the SR function. Note that using posterior predictive loss (Gelfand and Ghosh 1998) as a selection criterion, we confirmed that the performance of all four of these GP models were statistically equivalent within the range of the data. However, GP models are typically much worse at extrapolating than interpolating (Munch et al. 2005; Rasmussen and Williams 2006) and we therefore expect that these GP models will differ in their ability to accurately estimate lnα. To address this, we evaluated model

performance in terms of the average bias ($\mathrm{E}(\ln\alpha|\mathrm{data}) - \ln\alpha_{\mathrm{true}}$) and posterior variance ($\mathrm{V}(\ln\alpha|\mathrm{data})$) based on the analysis of 500 replicates for given σ^2 and $S_{\min}$.

The first alternative GP model is the model proposed by Munch et al. (2005), i.e.,

$$\ln R = f(\ln S) + \varepsilon$$

$$f \sim \mathrm{GP}(\mu', \Sigma')$$

where the prime on the mean and covariance functions is included to indicate that they are specified in terms of ln$S$. Specifically, the mean function is $\mu' = \ln\alpha$ and the covariance function was $\Sigma' = \tau^2 \exp\{-\phi|(\ln S - \ln S')/[\max(\ln S) - \min(\ln S)]|^2\}$ by analogy with Eq 5. The range of ln$S$ was standardized in the covariance function and the same priors for ϕ and τ^2 were used as in Eq 12. In the remainder of this paper we refer to this as the 'lnS' model.

The second GP model we used was the model given by Eqs 5-7, which is the GP model without conditioning $f(0)=\ln\alpha$. Prior specification was otherwise identical to that described for the 'linear' model. We refer to this prior specification as the 'S' model and included it primarily to evaluate the gain in posterior precision obtained by conditioning on $f(0)$. The third alternative GP model we tested was identical to the 'linear model' except that we used a constant mean function. That is, we replaced the mean function in Eq 6 with $\mu(S)=\ln\alpha$. Within the range of the data, this model should be identical to the 'linear' model. However, because estimation of lnα requires some extrapolation beyond the range of the data, this prior mean was included to assess the gain in posterior accuracy obtained by including a linear mean function. We refer to this as the 'constant' model.

We may think of this collection of GP models as supplying sequentially more information about the shape of the SR model. The 'lnS' model merely constrains recruitment to be positive. The 'S' model asserts that recruitment must be positive, and that it must be zero

when S is zero. The 'constant' model includes these constraints and specifies the slope at the origin as a parameter, but asserts no prior expectation about how recruits per spawner should change with stock biomass. Finally, the 'linear' model asserts the same constraints, specifies the slope at the origin as a parameter and asserts that recruits per spawner should decrease with stock biomass.

2-3. Results

For sake of clarity, we begin by describing results for a single simulated data set before moving on to the overall simulation. In the single example, the Ricker model was used to generate data with $\ln\alpha = \ln 4$, $S_{\min}=0.34$, and $\sigma^2=0.1$ (Fig. 1a). The credibility intervals based on variance of estimated $\ln\alpha$ indicate that the posterior variance and bias in the posterior mean are the smallest for the Ricker model, followed by the 'linear' model (Fig. 1b). Of the four GP models, the 'linear' model was the least biased and most precise, the 'constant' model was second best and the 'S' and the 'lnS' models performed equivalently poorly. All of these models gave better estimates than the BH model.

Turning now to the overall simulation, we found that averaging across both data-generating models and all combinations of $S_{\min}$ and σ^2, the 'linear' model produced the least biased estimates of $\ln\alpha$ (bias=-0.1829, variance=0.3517, Table 1c). Considering the Ricker and the BH data sets separately, the 'linear' model produced the least biased estimates for the Ricker data (Table 1a) and was second best for the BH data (Table 1b). The 'linear' model produced better estimates of $\ln\alpha$ for the Ricker data than for the BH data. When the generating model was the BH, estimates of $\ln\alpha$ by the 'linear' model were negatively biased (bias=-0.3659, Table 1b). Results for the bias are somewhat smaller than those obtained with the use of the Ricker model.

However, the magnitude of the variance was consistently larger for the 'linear' model than for the Ricker model (Table 1a,1b).

For all models, posterior variance in lnα increases with both S_{min} and σ^2 (Fig. 2,3). However, when S_{min} was small, bias in estimates of lnα were small at any σ^2 for all models. This result supports the intuitive assertion that an absence of data around the origin makes it difficult to generate accurate and precise estimates of lnα (Hilborn and Walters 1992; Shelton and Healey 1999).

In keeping with previous simulation results (Zhou 2007), we found that the Ricker model generated negatively biased estimates of lnα for both data sets (Table 1a,1b), whereas the BH model generated positively biased estimates (Table 1b). The degree of bias for BH estimates depended on both σ^2 and S_{min} in a more complicated way (Fig. 2e,3f), especially for the Ricker data (Fig. 2e). When $\sigma^2 = 0.1$, the magnitude of the bias increased monotonically with the increase of S_{min}. However, when $\sigma^2 = 0.8$, the magnitude of the bias increased with S_{min} up to 0.2 and decreased thereafter. Posterior uncertainty in lnα was also greater when estimated with the BH model than when the Ricker model was used, and generally increased with σ^2 and S_{min} (Fig. 2k,2l,3k,3l).

The alternative GP models did not perform as well as the 'linear' model. The 'constant' model performed well when data were available at low stock sizes, but its performance deteriorated as S_{min} increased. The performance of the other two GP models ('S' and 'lnS') was poor: posterior means were negatively-biased estimates for all combinations of S_{min} and σ^2 (Fig. 2a,2b,3a,3b) and the magnitude of the variance was much larger than that based on the conditional GP models (Fig. 2g,2h,3g,3h).

2-4. Discussion

Our simulation study showed that the 'linear' model generated the least biased estimates for $\ln\alpha$ of the four GP models for both the Ricker data sets and the BH data sets. The performance of the 'linear' model is relatively robust to noise and works at least as well as parametric models over a range of minimum stock sizes. It is worth recalling that the four GP models were statistically equivalent within the range of the data in that they gave nearly identical scores for model selection criteria (section 2-2-5). In light of this, we suggest that the use of model selection criteria to determine the 'best' estimate of $\ln\alpha$ (e.g., Barrowman et al. 2003; Wang and Liu 2006) may not be the best approach. Moreover, the 'constant' model provided good estimates of $\ln\alpha$ only when data were available close to the origin. This is because the GP models are typically worse at extrapolation than interpolation (Munch et al. 2005; Rasmussen and Williams 2006). In this respect, the 'linear' model, which has an additional term in the mean function to model linear density dependence, does a better job of extrapolating to the origin.

Performance of the Ricker model is nearly as good as that of the 'linear' model in terms of bias, implying that there may be no need for using the apparently complex 'linear' model. We expect, however, that the 'linear' model will outperform the Ricker model when the generating models are more complex, such as models that include depensation (i.e., Allee effects) (Quinn and Deriso 1999; Courchamp et al. 2008).

To illustrate this point, we conducted a much smaller simulation study using the Saila-Lorda (SL) model to generate the data ($R=\alpha S^{\gamma}\exp(-\beta S+\varepsilon)$, $\varepsilon\sim N(0,\sigma^2)$, α=11.5416, β=2.5330, γ=2, Quinn and Deriso 1999). We chose α and β, so values of the carrying capacity for the SL model and the Ricker model used in this study are same and the linear approximation of the SL model at the carrying capacity is identical to the Ricker model. The data sets were generated with the

SL model using the same range for stock sizes and σ^2 used for the Ricker and the BH data sets (Fig. 2,3). Note that for $\gamma \neq 1$ the true slope at the origin for the SL model is simply 0 regardless of the value of lnα. We therefore estimated the slope at S=0.01 for which the true value is lnα=-2.1845. This simulation showed that the 'linear' model performed better than the Ricker model did (Table 2, Fig. 4) particularly when data were available at smaller stock sizes. Averaging over the simulation, the bias and variance in the 'linear' model were 2.5427 and 0.3912, respectively, whereas those in the Ricker model were 2.8836 and 0.1395 (Table 2). In our experience, this is a general property of parametric models – they produce greater apparent certainty at the cost of increased bias. Moreover, the 'linear' model significantly outperformed the Ricker model at smaller minimum stock sizes. In light of the fact that the true model is never known and that the underlying dynamics may be complex, the 'linear' model may be preferable for estimating lnα despite the apparent increase in computational complexity.

Extensions

The modeling framework used in this study is specifically designed to obtain an estimate for lnα for a single stock. This is adequate if SR relationships of different stocks are mutually independent. However, with mixing among populations (Bohonak 1999; Campana 1999) or similarity of environmental characteristics, this approach may be inefficient or inappropriate. Although the process error term ε in Eq 4 is intended to account for these effects implicitly, it would be more desirable to include environmental effects explicitly. Several nonparametric methods have been developed to include environmental covariates in a SR relationship (Chen and Ware 1999; Chen et al. 2000; Chen and Irvine 2001; Wang et al. 2009). Extending the

nonparametric Bayesian method to account for environmental effects while simultaneously providing robust estimates of $\ln\alpha$ is an important direction for future work.

In addition, it is reasonable to assume the presence of some common characteristics among different stocks of a single species. Meta-analysis is a common approach to obtaining common characteristics from different data sets. In the context of a SR relationship, Myers et al. (1999) and Myers et al. (2001) used the Ricker model and the BH model, respectively, to conduct across-species comparison of maximum annual reproductive rates by obtaining species-specific estimates of the slope at the origin. In spite of the diversity of the fish life histories and their habitats, Myers et al. (1999) obtained the general conclusion that the maximum annual reproductive rates for fish ranges only from 1 to 7. However, this conclusion may be highly conditional on the choice of a parametric model, and a more flexible approach may be needed to account for possibility that the shape of the SR relationship may vary across species and across stocks. To address this possibility, our SB method could be extended in a hierarchical manner to enable meta-analysis of annual reproductive rates without specific SR model forms.

2-5. Tables

Table 1. The performance of the six models for estimating lnα. **a**-**b**: For the Ricker data (a) and the BH data (b), bias and variance in estimated lnα were averaged over the number of replicates, the noise level, and the minimum stock size. **c**: Bias and variance were further averaged over data-generating models.

(a) The Ricker data

	lnS	S	Constant	Linear	BH	Ricker (true)
Bias	-1.0021	-1.0000	-0.5116	0.0002	0.5943	-0.0010
Variance	1.1300	1.1301	0.3666	0.3534	0.7774	0.1315

(b) The BH data

	lnS	S	Constant	Linear	BH (true)	Ricker
Bias	-1.1672	-1.1657	-0.7768	-0.3659	0.0605	-0.4680
Variance	1.0042	1.0073	0.3085	0.3500	0.6171	0.1324

(c) Average of the two data-generating model

	lnS	S	Constant	Linear	BH	Ricker
Bias	-1.0847	-1.0829	-0.6442	-0.1829	0.3274	-0.2345
Variance	1.0671	1.0687	0.3376	0.3517	0.6973	0.1319

Table 2. The performance of the 'linear' model and the Ricker model when data sets are depensatory. Bias and variance in estimated lnα were averaged over the number of replicates, the noise level, and the minimum stock size.

	Linear	Ricker
Bias	2.5427	2.8836
Variance	0.3912	0.1395

2-6. Figures

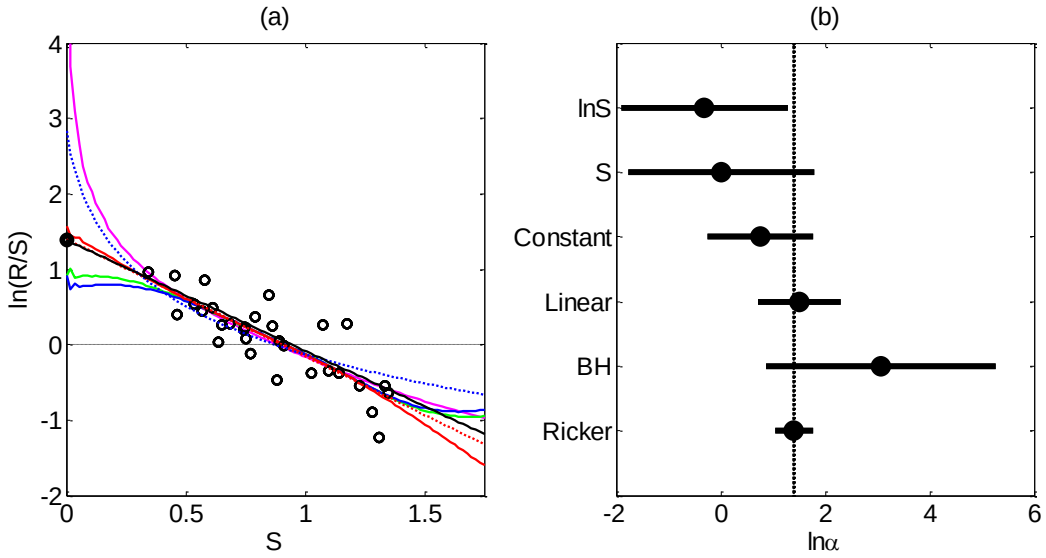

Figure 1. An example result. **a:** The Ricker model (black) was used to generate data (lnα=ln4, S_{min}=0.34, and σ^2=0.1). The true value of lnα is indicated by the black dot. Means of posterior predictive distributions of the four GP models and the two parametric models are plotted: 'lnS' model (magenta), 'S' model (green), the 'constant' model (blue), the 'linear' model (red), the BH model (blue dash), and the Ricker model (red dash). Note that within the range of the data all models seem to fit equally well, but only the 'linear' and the Ricker models come close to the correct value of lnα. **b:** Bias and credibility intervals of estimated lnα. Deviation of posterior means (black dot) from the true lnα (vertical dash) indicates magnitude of bias in estimated lnα. The credibility intervals (horizontal black solid) are based on posterior variances of lnα. The intervals cover $\pm$2 standard deviation of the estimated lnα from the mean of estimated lnα.

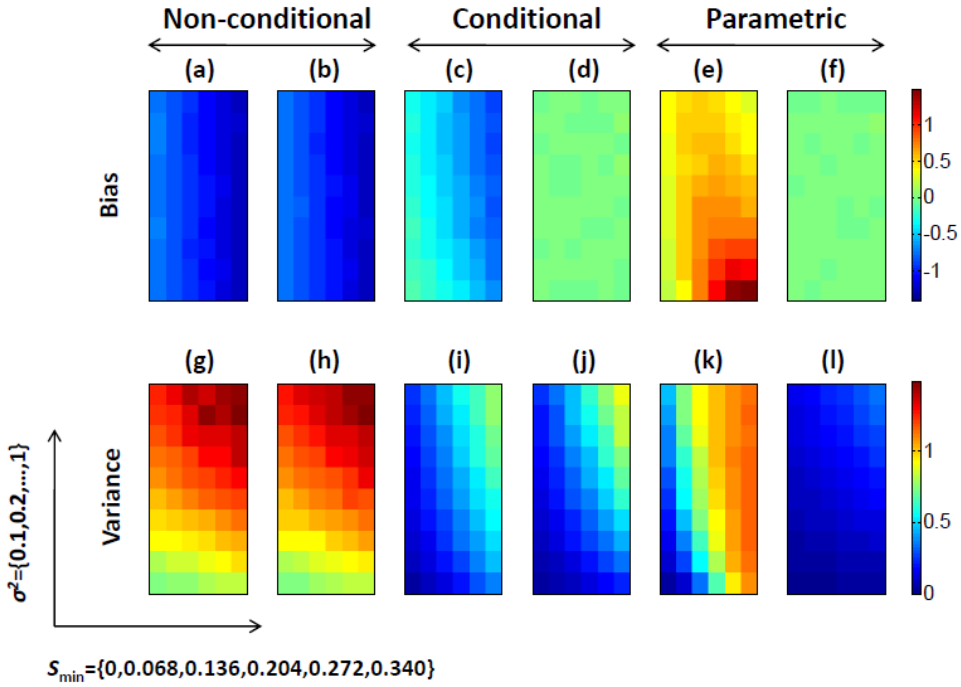

Figure 2. The results of the comprehensive analysis on the Ricker datasets. **a-f:** The bias in the estimates for lnα using (a) the 'lnS' model, (b) the 'S' model, (c) the 'constant' model, (d) the 'linear' model, (e) the BH model (the false model), and (f) the Ricker model (the true model). **g-l:** The variance in the estimates for lnα using (g) the 'lnS' model, (h) the 'S' model, (i) the 'constant' model, (j) the 'linear' model, (k) the BH model (the false model), and (l) the Ricker model (the true model). x axis is S_{min}={0,0.068,0.136,0.204,0.272,0.340} and y axis is σ^2={0.1,0.2,…,1}.

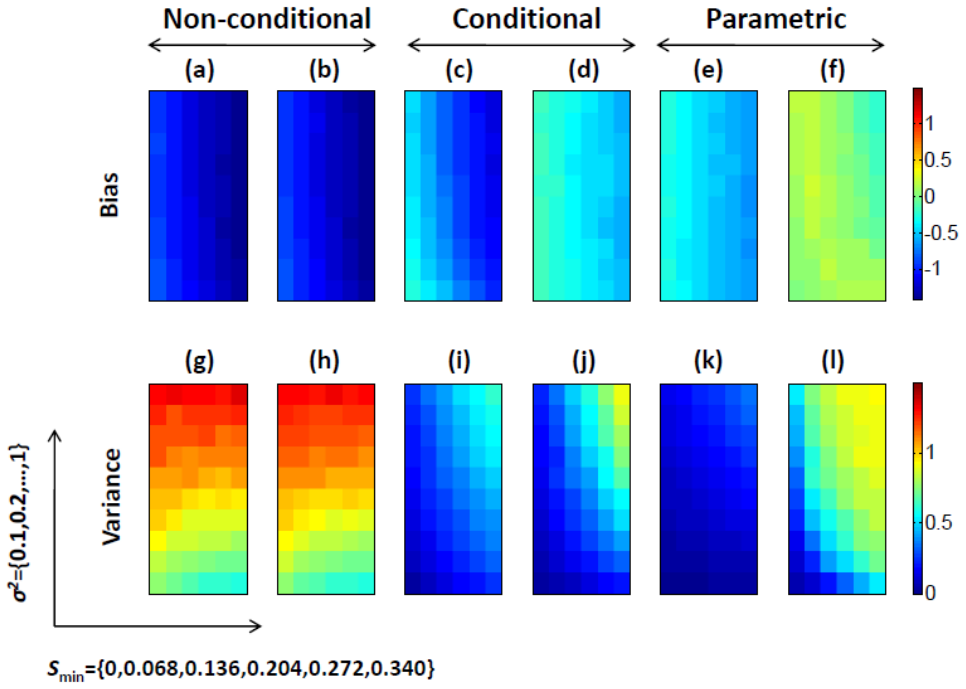

Figure 3. The results of the comprehensive analysis on the BH datasets. **a-f:** The bias in the estimates for lnα using (a) the 'lnS' model, (b) the 'S' model, (c) the 'constant' model, (d) the 'linear' model, (e) the 'Ricker' model (the false model), and (f) the BH model (the true model). **g-l:** The variance in the estimates for lnα using (g) the 'lnS' model, (h) the 'S' model, (i) the 'constant' model, (j) the 'linear' model, (k) the Ricker model (the false model), and (l) the BH model (the true model). x axis is S_{min}={0,0.068,0.136,0.204,0.272,0.340} and y axis is σ^2={0.1,0.2,…,1}.

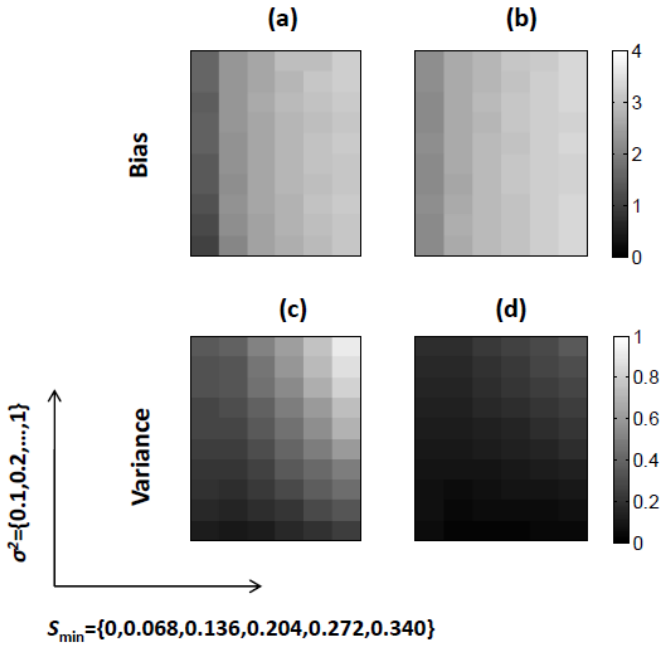

Figure 4. The performance of the 'linear' model and the Ricker model when data sets are depensatory. The data-generating model was the SL model with a multiplicative log normal error $\exp(\varepsilon)$ ($R=\alpha S^{\gamma}\exp(-\beta S+\varepsilon)$, $\varepsilon\sim N(0,\sigma^2)$, α=11.5416, β=2.5330, γ=2). Given γ=2, we chose α and β so that the carrying capacity for the SL model and the Ricker model used in this study are the same, and the linear approximation of the SL model at the carrying capacity is identical to the Ricker model. The data sets were generated using the same range for stock size and σ^2 used for the Ricker and the BH data sets. Because $\ln\alpha$ in the SL model is negative infinite, we approximated it by substituting S=0.01 in the SL model, and obtained $\ln\alpha$=-2.1845. **a-b:** The bias in the estimates for $\ln\alpha$ using (a) the 'linear' model and (b) the Ricker model. **c-d:** The variance in the estimates for $\ln\alpha$ using (c) the 'linear' model and (b) the Ricker model.

Chapter 3

A semiparametric Bayesian model for detecting Allee effects

Key words

Allee effects, depensation, Gaussian process, semiparametric Bayesian modeling

Abstract

The importance of Allee effects has long been recognized both in theoretical studies of population dynamics and in conservation sciences. Although the necessary conditions for Allee effects to occur (e.g., difficulty in finding mates and mortality driven by generalist predators at low density, etc.) would seem to apply to many species, evidence for Allee effects in natural populations is equivocal at best. This apparent scarcity might be an artifact driven by poor power to detect them with traditional parametric models. To circumvent this potential problem, we developed a semiparametric Bayesian model based on a Gaussian process prior. We validated the model using simulated data and applied it to three example datasets.

3-1. Introduction

Allee effects, the reduction of per capita population growth rates with the decrease of population size, have long been recognized in theoretical studies of population dynamics and hypothesized as potential contributors to population extinction (Courchamp et al. 2008). In fisheries science this phenomenon is also known as depensation, defined as the decrease in per-capita recruitment with decreasing spawner abundance at low stock levels (Quinn and Deriso 1999).

Theoretical studies suggest important implications of Allee effects for conserving and managing wild populations. Extinction probabilities for endangered species (Boukal and Berec 2002; Dennis 2002), vulnerability to invasion by introduced species and risk of disease outbreak (Tayler and Hastings 2005; Tobin et al. 2011), robust restoration programs for collapsed populations (Grevstad 1999; Deredec and Courchamp 2007; Armstrong and Wittmer 2011), and optimum harvesting rates for the sustainable use of wild populations (Lande et al. 1994), are all dependent on whether or not Allee effects are incorporated in model analysis. Allee effects may also offer an explanation for the ineffectiveness of fishing moratoria to rebuild collapsed fisheries (Swain and Sinclair 2000; Walters and Kitchell 2001).

Several mechanisms contribute to generating Allee effects, including increased difficulty in finding mates (Gascoigne et al. 2009), increased mortality driven by generalist predators (Gascoigne and Lipcius 2004), and decreased fitness due to inbreeding depression (Willi et al. 2005). Each of these potential mechanisms has been observed at reduced population sizes (Berec et al. 2007; Courchamp et al. 2008; Gascoigne et al. 2009; Kramer et al 2009). Because the conditions for Allee effects to occur seem likely to apply in many species, we would expect Allee effects to manifest at the population level, referred to as 'demographic' Allee effects (Stephens and Sutherland 1999). However, evidence for the presence of demographic Allee effects (hereafter Allee effects) is equivocal at best. Previous analyses of ecological time series for both terrestrial and aquatic species (Saether et al. 1996; Sibly et al. 2005; Gregory et al. 2010) and fisheries data (Myers et al. 1995; Liermann and Hilborn 1997; Chen et al. 2002; Barrowman et al. 2003; Nash et al. 2009) found limited evidence for Allee effects, leading to a general consensus that demographic Allee effects are quite rare.

However, there are two potential pitfalls regarding previous methods for detecting Allee effects. First, the conclusions of the previous analyses are clearly conditional on the parametric model used to test for Allee effects. This is particularly important for noisy ecological data because many different models may fit equally well (or poorly) but produce qualitatively different predictions (e.g., Wood and Thomas 1999). Second, even when the correct model is *known*, Allee effects may be difficult to detect in noisy, short data sets (Shelton and Healey 1999). Using simulated data generated by an Allee effects model (the sigmoid Beverton-Holt model), Shelton and Healey (1999) demonstrated that likelihood ratio tests favored the true Allee effects model over the non-Allee effects model (the BH model) only when (1) simulated data clearly show the shape of the true Allee effects model, or (2) large samples ($n>60$) are available.

Because we do not know the correct model and data clearly exhibiting Allee effects are rarely available, we hypothesize that the empirical rarity of Allee effects may be an artifact driven by poor power to detect them with traditional parametric models. To circumvent this limitation, we developed a semiparametric Bayesian (SB) model using a Gaussian process (GP) prior (Munch et al. 2005, Rasmussen and Williams 2006) to construct an index for assessing the presence of Allee effects. While some non/semi-parametric models are available for modeling simple population dynamics (e.g., Evans and Rice 1988; Cook 1998; Bravington et al. 2000; Munch et al. 2005), none of these directly addressed the detection of Allee effects. We validated the model using simulated data and applied the method to data for three different herring populations.

3-2. Methods

We begin this section by developing a general approach to modeling Allee effects and Gaussian process (GP) modeling of density dependence. We then develop a semiparametric Bayesian (SB) approach to determining the presence of Allee effects. Finally, we describe simulation studies used for model validation and three herring data used for case studies. Mathematical details are given in Appendices B, C, and D.

3-2-1. The Allee effects model

The relationship between adult (A) and juvenile (J) biomass can be written as:

$$J = A\exp[f(A)] \tag{1}$$

where the arbitrary function, $f(A)$, determines the form of density dependence (Quinn and Deriso 1999; Courchamp et al. 2008). For mathematical convenience, we re-write Eq 1 using $y = \ln(J/A)$, and work with the log-transformed version of Eq 1,

$$y = f(A). \tag{2}$$

Allee effects occur when $f(A) < 0$ for some small adult biomass so that juvenile biomass falls below the level required for a population to persist. If this is the case, then there must also be some small adult biomass for which $f(A)$ is increasing (i.e., a particular value of A where $f'(A) \equiv df/dA > 0$) otherwise persistence would be impossible at any adult biomass (Quinn and Deriso 1999; Courchamp et al. 2008). Therefore, general conditions for the presence of Allee effects are:

$$f(A) \leq 0, f'(A) > 0 \tag{3}$$

for some small values of A (see Fig. 1 for an illustration). Eq 3 indicates that there is a particular adult biomass below which $f(A) = 0$ is met, which we define as A_T. Since a population whose

adult biomass is below A_T fails to maintain the current adult biomass, the population is considered to be at the edge of extinction when reduced below A_T (Quinn and Deriso 1999; Courchamp et al. 2008). For this reason, A_T is called an Allee effects threshold (Courchamp et al. 2008) or a critical depensation biomass (Quinn and Deriso 1999). The sigmoid Beverton-Holt (SBH) model (Myers et al. 1995) and the Saila-Lorda (SL) model (Saila et al. 1988) are common parametric models incorporating Allee effects, though other choices are possible (Liermann and Hilborn 2001; Boukal and Berec 2002).

In practice, Eqs 1 and 2 are only approximate. In keeping with a standard analysis of population time series (e.g., Myers et al. 1995; Gregory et al. 2010), we append an additive noise term ε to Eq 2, which is normally distributed with the mean 0 and the variance σ^2.

3-2-2. Modeling $f(A)$ with a GP prior

Our semiparametric framework involves Bayesian inference for $f(A)$ starting from a GP prior, and uses the inference for $f(A)$ for detecting Allee effects. A GP prior is a generalization of the multivariate normal distribution to spaces of random functions (i.e., A is, in principle, a continuous variable), and analogously, the distribution is specified in terms of a mean function $\mu(A)$ and a covariance function $\Sigma_{f,f}(A, A')$ (Rasmussen and Williams 2006). A GP prior generates random functions $f(A)$ to model density dependence. The application of a GP prior to Bayesian analysis was introduced by O'Hagan and Kingman (1978), and a GP prior was applied to modeling density dependence by Munch et al. (2005). Rasmussen and Williams (2006) provide an excellent introduction to GP-based inference.

Since the linear model is a common starting point for modeling density dependence (Myers et al. 1999; Sibly et al. 2005; Gregory et al. 2010), we assumed linearity in the prior

mean function. Because we have no *a priori* reason to assume that the uncertainty of $f(A)$ or its curvature vary predictably with A, we used an isotropic covariance function. Specifically, we use the GP prior:

$$f(A) \sim \mathrm{GP}\left[\mu(A), \Sigma_{f,f}(A, A')\right] \tag{4}$$

$$\mu(A) = \ln\alpha + \beta A/\max(A)$$

$$\Sigma_{f,f}(A, A') = \tau^2 \exp\left[-\phi \left|\frac{A - A'}{\max(A)}\right|^2\right],$$

where $\ln\alpha$ and β are unbounded while τ^2 and ϕ are strictly positive. In this parameterization, τ^2 determines the vertical range of sampled $f(A)$ and ϕ determines its smoothness; a GP with a large (small) ϕ generates realizations of $f(A)$ which contain many (few) inflection points over A. Note that this choice for $\mu(A)$ and $\Sigma_{f,f}(A, A')$ does not severely limit the range of possible functional forms in the posterior within the range of the data (Munch et al. 2005; Rasmussen and Williams 2006); almost any functional shape clearly visible in the data may be recovered. We specified reference priors for $\ln\alpha$ and β and minimally informative priors for τ^2 and ϕ (Appendix B). We fit the GP prior using Metropolis sampling after marginalizing over $f(A)$ (Munch et al. 2005, Rasmussen and Williams 2006). Details for prior specification and posterior inference are given in Appendix B.

3-2-3. Allee effects detection

The core idea of this paper is that we can use the GP machinery to calculate the probability that Allee effects are present. Specifically, we are interested in evaluating the probability that some adult biomass satisfies the conditions for the presence of Allee effects laid out in Eq 3, i.e., $\Pr[f(A) \leq 0, f'(A) > 0 | \mathrm{data}]$. To simplify notation in what follows, all the

parameters in the model are collected in the vector $\boldsymbol{\Theta} = \{\ln\alpha, \beta, \phi, \tau^2, \sigma^2\}$. We note that because the derivative of a GP is also a GP (See Appendix C and Rasmussen and Williams 2006), the joint distribution for $f(A)$ and $f'(A)$ at a specific A given the parameters, i.e., $\Pr[f(A), f'(A)|\boldsymbol{\Theta}, \text{data}]$, is bivariate normal (see Appendix C). Therefore, to calculate the posterior probability of the presence of Allee effects given $\boldsymbol{\Theta}$ at A, we evaluate the cumulative bivariate normal.

We are of course more interested in the posterior inference of Allee effects that are exclusively conditioned on data and not dependent on specific choice of $\boldsymbol{\Theta}$. However, since these probabilities, $\Pr[f(A) < 0, f'(A) > 0|\text{data}]$, are not analytically tractable, we obtained them by Monte Carlo integration over the posterior for $\boldsymbol{\Theta}$ and evaluated them over the entire range of $A \in [0, max(A)]$. For more details on these calculations, see Appendices C and D.

Our assessment framework for determining the presence of Allee effects is simply based on comparison of the prior and the posterior probability for the presence of Allee effects, $\Pr[f(A) < 0, f'(A) > 0|\text{data}]$, which is clearly a function of A. Since this probability is most relevant to Allee effects at small A, we used the probability evaluated at $A = 0$ as an index, π, for the presence of Allee effects:

$$\pi = \Pr[f(0) \leq 0, f'(0) > 0|\text{data}]. \quad (5)$$

In light of our prior specification, the value of π prior to collecting any data is 0.25, providing a convenient benchmark against which to compare specific results (see Appendix C). Thus, a given data set suggests that Allee effects are present if $\pi > 0.25$.

3-2-4. Simulation study

We tested our method with simulated data. Because the strength of Allee effects, the noise level in data, and the data availability at low adult biomass should influence our ability to correctly assess the presence of Allee effects (Hilborn and Walters 1992; Shelton and Healey 1999), our simulation study was designed to assess these factors comprehensively. For each treatment combination (i.e., Allee effect strength, noise level, and minimum adult biomass) we generated 500 replicate data sets. For each simulated data set, we set the total number of observations to 30, which is representative of many ecological data sets.

We used the Saila-Lorda (SL) model (Saila et al. 1988), $J = \alpha A^{\gamma} \exp(-\beta A)$, to generate data with and without Allee effects (Table 1). The parameter γ controls the strength of Allee effects. We used three different strength levels: $\gamma = 1$ for data with negative density dependence (the Ricker model, hereafter 'no effect'), $\gamma = 1.5$ for data with mild Allee effects ('mild'), and $\gamma = 2$ for data with strong Allee effects ('strong'). In the 'no effect' case ($\gamma = 1$), we used a value of 4 for α and set $\beta = \alpha/e = 1.47$. For the 'mild' and 'strong' cases we parameterized our simulation to isolate the influence of Allee effect strength on our ability to detect Allee effects. Specifically, we set parameters in the SL model so that the adult biomass which can be replaced by the juvenile biomass (i.e., the largest A that satisfies $A = J$) and the slope, dy/dA at that adult biomass were constant across all three models. The list of parameters used is given in Table 1.

Variability in J was modeled by a multiplicative log-normal noise without serial autocorrelation, $J = \alpha A^{\gamma} \exp(-\beta A + \omega)$, where $\omega \sim \mathrm{N}(0, \sigma_J^2)$ and σ_J^2 is the variance. We used σ_J^2 over the interval 0.1 to 1.

To evaluate model performance with respect to the availability of data at low adult biomass independently of the range of adult biomass values, we sampled A from a uniform distribution with constant width and variable minimum adult biomass. Preliminary analysis of data for Atlantic cod (*Gadus morhua*) indicates that the range of observed adult biomass is typically on the order of 1.5 times the adult biomass that generates the maximum juvenile biomass (see chapter 2). In the 'no effect' model with $\alpha = 4$ and $\beta = 1.47$, this adult biomass is given by 0.68. Therefore, by multiplying this value with 1.5, we obtained 1.02 as the width and then set the minimum adult biomass for this distribution as a proportion of 0.68, ranging from 0 to 0.34.

We compared the performance of our SB approach with the likelihood-based parametric approach in terms of type I (false positive detection of Allee effects) and type II (false negative detection of Allee effects) error rates. In keeping with previous parametric assessments of Allee effect frequency, we used the likelihood ratio to test for Allee effects, by comparing the fit of the SL model to the fit of the Ricker model (i.e., the SL model with $\gamma = 1$). To do so, we compared the likelihood ratio to a χ^2 distribution with 1 df and concluded that Allee effects are present if the nominal confidence level exceeded p=0.05. To evaluate the sensitivity of our conclusions to parametric model choice, we also conducted likelihood ratio tests comparing the fit of the SBH model where $J = \alpha A^{\gamma}/(1 + \beta A^{\gamma})$ to the standard Beverton-Holt (BH) model (i.e., when $\gamma = 1$). For the SB model, we concluded that Allee effects were present whenever the posterior value for π exceeded the prior of 0.25. For each of these approaches (SL, SBH, and SB), we estimated error rates from the 500 replicates for each parameter combination. All calculations were carried out using code written in Matlab 7 (The MathWorks, Nattick, MA).

3-2-5. Herring data

To illustrate application of this method to real data, we analyzed three different Atlantic herring (*Clupea harengus*) data sets from the 'Stock Recruitment Database' (http://www.mscs.dal.ca/~myers/welcome.html). We used data on Iceland spring spawner (ICE, n=23, 1947-1969), Downs stock (DOWN, n=65, 1923-1987), and Georges bank (GB, n=15, 1961-1975). In keeping with previous work (Myers et al. 1995), the raw juvenile biomass data (in the unit of the number of individuals) were multiplied by weight per individual so that y was dimensionless.

3-3. Results

3-3-1. Simulation results: case studies

For clarity, we begin by describing a single set of simulations before describing the results of the broader simulation study. In this illustrative example (Figs. 2,3), we examined model performance under 'no', 'mild', and 'strong' Allee effects fixing zero minimum adult biomass and $\sigma_J^2 = 0.5$. In each case, the SB fit reasonably recaptures the shape of the data-generating models (Figs. 2a,b,c). More importantly, the probability of the presence of Allee effects clearly corresponds to the truth in the simulated data. In the 'no effect' case the probability is zero for all points close to the origin (Fig. 2d). In the 'strong' effects case, there is a clear region in which the probability is close to 1 (Fig. 2f). In the 'mild' case, there is a peak in the probability at the origin, but with wide confidence intervals. In these examples, the probability for the presence of Allee effects, π, generated correct assessment for the 'no effect' and 'strong' data, while the assessment for 'mild' data was somewhat more ambiguous (Fig. 3).

3-3-2. Allee effects detection frequency

We turn now to summarizing the results of the simulation in general. Overall, averaging across data-generating models, noise levels, and the minimum adult biomass, the SB model is the best model for correctly assessing for the presence of Allee effects (Table 2). The error rate for the SB model is 0.49, whereas those for parametric models were 0.53 (SL) and 0.54 (SBH), respectively. When type I errors (false positive) and type II errors (false negative) are considered separately, the SB model performed best when data were 'no effect' and 'strong', followed by the SL and the SBH model (Table 2). When the data are 'mild', the three models performed equivalently, with a slight advantage for the SL model, followed by the SB model and the SBH model.

To compare the performance of the SB model with parametric alternatives in detail, we generated Fig. 4 using subsets of the comprehensive analysis to show how the error rates were affected by the data-generating models, the noise level, and the minimum adult biomass. For 'no effects' cases, the type I error rate for all three methods is quite low overall (Figs. 4a,d,g,j). With data close to the origin (0 for the minimum adult biomass) and the low noise level in data ($\sigma_f^2 = 0.1$), the SB model is the only method that showed 0 error rate. The error rate for the SL model (0.02) is within acceptable levels, but that for the SBH model (0.18) is more than 3 times the nominal 0.05 level.

For 'mild' and 'strong' cases, the type II error rates for all three models are greater and clearly increased with minimum adult biomass. In keeping with previous results (Shelton and Healey 1999), the type II error rate is larger in the 'mild' case than in the 'strong' case. In addition, as the noise level and minimum adult biomass increase, detection probability goes down significantly and the performance of the parametric models is equivalent. The SB model

performed better than the parametric models in general, particularly when the noise level was large and was only outperformed by parametric alternatives at low noise ($\sigma_f^2 = 0.1$).

3-3-3. Empirical results: herring data

Using π calcualted for herring data, we found evidence for the presence of Allee effects in Iceland spring spawner population (ICE) and in the Georges bank population (GB), but no evidence in the Downs stock population (DOWN) (Fig. 6). ICE is the population in which Allee effects was found using the SBH model (Myers et al. 1995). The confidence intervals in π show that the results for ICE and GB are ambiguous, suggesting that Allee effects are 'mild'. However, note that these probabilities are ambiguous for GB, probably due to the limited sample size ($n = 15$).

3-4. Discussion

In the context of Allee effects detection, type I (false positive) and type II (false negative) errors are not equivalent: the cost of a type I error is reduced harvesting on a viable population while the cost of a type II error is extinction (Table 3) (e.g., Courchamp et al. 1999; Stephens and Sutherland 1999; Mieszkowska et al. 2009). Our results suggest that the SB model could reduce chance of overexploitation and population collapse due to making a type II error: the SB model is clearly better at detecting Allee effects when present compared to parametric alternatives, including the true model, especially when 'strong' Allee effects are present. Moreover, the SB approach is effective regardless of the 'true' model. This alone should make it broadly applicable in ecology where the underlying dynamics are rarely certain. That said, the success of the

approach is tempered somewhat by the fact that type II error rates were still above 50% for most cases, indicating the need for caution.

In this study, the SB approach to detecting Allee effects was based on comparison of the probability for the presence of Allee effects, π, with 0.25 detection threshold which emerges from the specification of the prior. Using this threshold, the SB approach reduced the chance of making a type II error compared with parametric models, but the error rate was still quite high. Because of asymmetric cost of incorrect assessment for the presence of Allee effects (Table 3) and need for precautionary approaches to managing natural populations (e.g., Hilborn et al. 2001), it may be desirable to set the detection threshold at some lower value in order to further reduce the chance of making a type II error. In broad terms, a precautionary threshold might allow for a greater probability of a type I error in order to avoid rejecting Allee effects when they are hard to detect. Of course, adopting an excessive safety margin would result in unnecessary losses to society as well (e.g., Hilborn et al. 2001) and we agree with many prior studies that a decision-theoretic approach (Berger 1985; Francis and Shotton 1997; Punt and Hilborn 1997; Wade 2000; Fenichel et al. 2008) should be taken to determine the most reasonable threshold level. This process usually requires considerable discussion between scientists, environmental practitioners, and local communities and is beyond the scope of the present paper.

Previous studies have concluded that Allee effects are quite rare in natural populations. Using parametric models and likelihood ratio tests, Gregory et al. (2010) analyzed 1198 data that include both terrestrial and aquatic species and Myers et al. (1995) analyzed 129 data on commercially harvested fish species. These studies concluded that Allee effects appear in <1.1% and <2.3% of populations, respectively. Given the results of our simulation study, however, we

suspect that Allee effects are more prevalent than currently believed. Re-analysis of these data with a more sensitive tool such as the SB model developed here seems warranted.

3-5. Tables

Table 1. Parameters for the data-generating models, $J = \alpha A^{\gamma} \exp(-\beta A)$. A_T is not available in 'no effect' model because the model shows density dependence without Allee effects.

	α	β	γ	A_T
No effect	4	1.4712	1	N/A
Mild	6.7964	2.0023	1.5	0.0238
Strong	11.5416	2.533	2	0.1163

Table 2. The error rates of the SB model, the SL model, and the SBH model in assessing for the presence of Allee effects. 'Average' is the error rate averaged over the noise level, the minimum adult biomass, and data-generating models. Error rates for the three models in 'no effects', 'mild', and 'strong' data are also shown. The number indicated with bold type indicates the best model in each category.

	Average	**No effects**	**Mild**	**Strong**
SB model	**0.4890**	**0.0265**	0.8572	**0.5832**
SL	0.5271	0.0284	**0.8508**	0.7021
SBH	0.5432	0.0416	0.8580	0.7301

Table 3. The consequence of incorrect assessment for the presence of Allee effects on populations.

		A true form of density dependence	
Assessment		**No effects**	**Allee effects**
	No effects	**Rebuild**	**Type II error (Extinction)**
	Allee effects	**Type I error (Rebuild)**	**Rebuild**

3-6. Figures

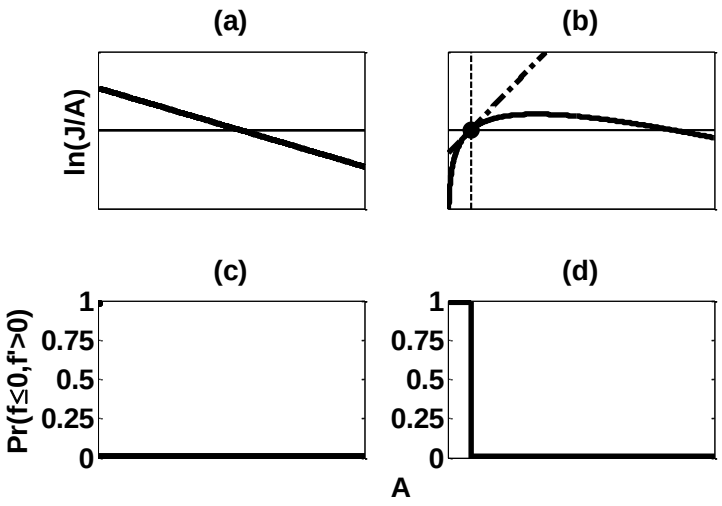

Figure 1. **a**: An example of a function for density dependence without Allee effects [soild line]. **b**: An example of a function with Allee effects [solid line], the Allee effects threshold A_T [dot], and the slope of the example function at A_T [broken line]. **c**: The probability for the presence of Allee effects, $\Pr[f(A) \leq 0, f'(A) > 0]$, obtained from the example function used in (a). **d**: The probability for the presence of Allee effects obtained from the example function used in (b).

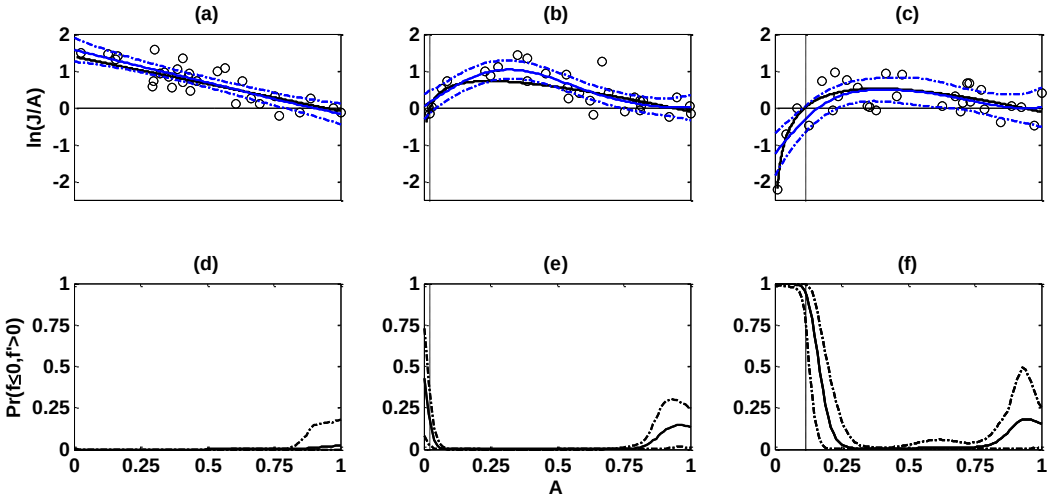

Figure 2. An illustration of the SB approach to detecting Allee effects using simulated data with 0 for minimum adult biomass and $\sigma_J^2 = 0.5$. The data models used to generate simulated data were the 'no effect' model ($\gamma = 1$ in the SL model) (a,d), the 'mild' Allee effects model ($\gamma = 1.5$ in the SL model, $A_T = 0.024$) (b,e), and the 'strong' Allee effects model ($\gamma = 2$, $A_T = 0.12$) (c,f). **a-c**: Fit of the GP model to simulated data. We plotted the true functions [solid black line], simulated data [circles], the mean [solid blue line] and the 95% confidence intervals [broken blue line] of the posterior predictive $f(A)$. The true A_T is indicated by the vertical dotted line. **d-f**: The posterior probability for the presence of Allee effects. We plotted the mean [solid line] and the 95% confidence intervals of the posterior probability [broken line].

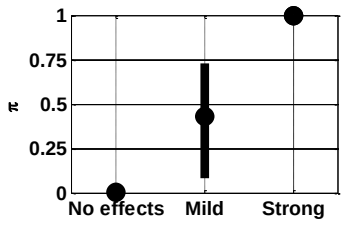

Figure 3. The probability for the presence of Allee effects at zero adult biomass level, π, for data with three different Allee effects strength. We plotted the probability [dot] and the 95% confidence intervals [solid line].

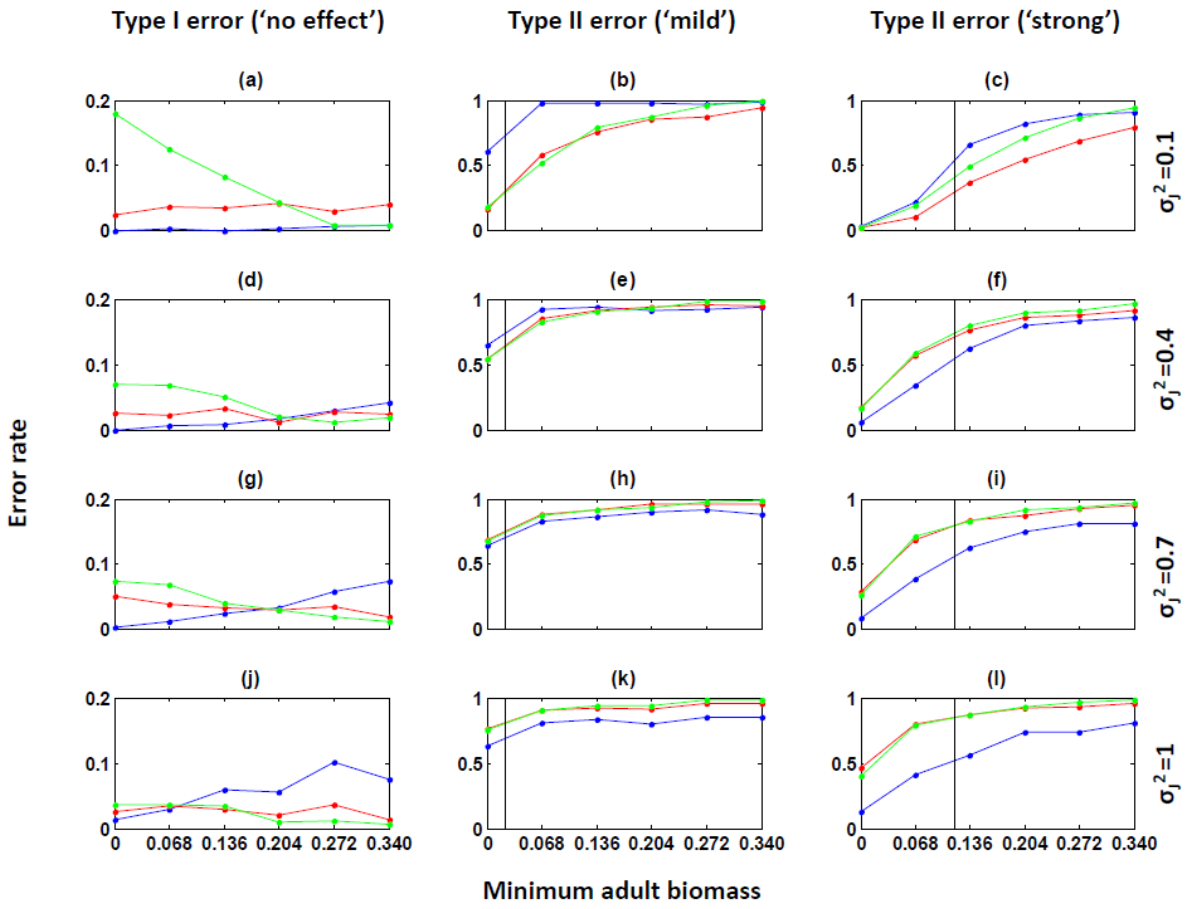

Figure 4. Frequency of making incorrect assessment for the presence of Allee effects. The left column describes results for data without Allee effects ('no effects'). Hence we focus on a type I error (false positive). The middle and right columns describe results for 'mild' and 'strong' Allee effects and therefore we focused on a type II error (false negative). In each panel, the horizontal axis is minimum adult biomass in simulated data and the vertical axis is the frequency of making an incorrect assessment for the presence of Allee effects. Rows of the plots correspond to noise levels $\sigma_j^2 = \{0.1,0.4,0.7,1\}$. Blue lines give error rates for the SB model, the red and green lines give error rates for the SL and the SBH likelihood ratio tests respectively. In the middle and right columns, the vertical line indicates values of Allee effects thresholds A_T ($A_T = 0.024$ for 'mild' Allee effects and $A_T = 0.12$ for 'strong' Allee effects).

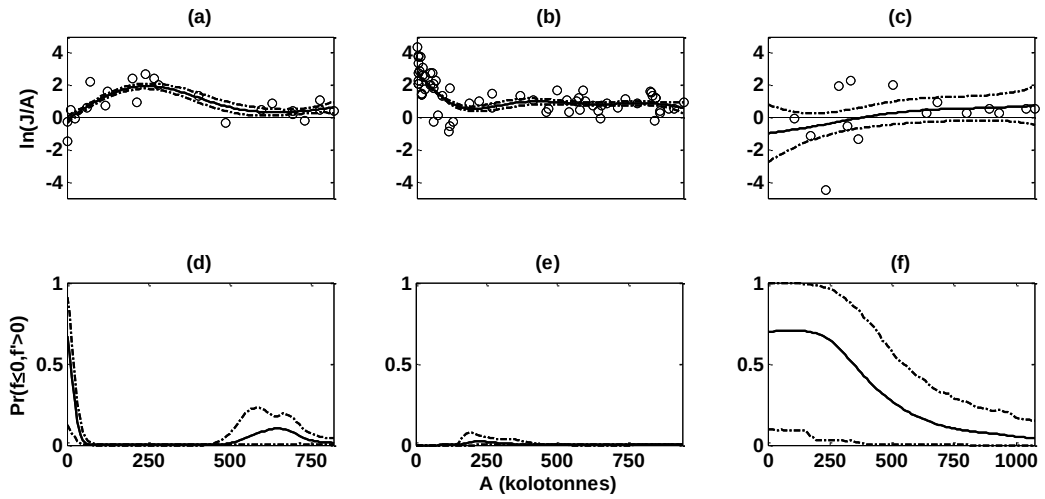

Figure 5. Data analysis on three herring data. They are ICE (a,d), DOWN (b,e), and GB (c,f). **a-c**: The posterior predictive distributions for $f(A)$ were obtained for checking fits of the SB model. We plotted data [circles] and the mean [solid line] and the 95% confidence intervals of the posterior predictive $f(A)$ [broken line]. **d-f**: The posterior probability for the presence of Allee effects. We plotted the mean [solid line] and the 95% confidence intervals of the posterior probability [broken line].

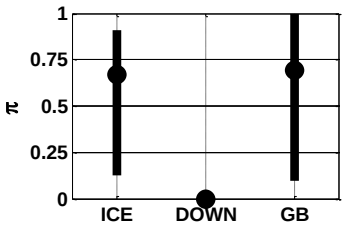

Figure 6. The probability for the presence of Allee effects at zero adult biomass level, π, for three herring data, ICE, DOWN, and GB. We plotted the probability [dot] and the 95% confidence intervals [solid line].

Chapter 4

The limits to productivity: Semiparametric Bayesian estimation of reproductive rates at low densities

Key words

Allee effects, Bayesian modeling, depensation, Gaussian processes, reproductive rate, stock-recruitment relationship

Abstract

The maximum annual reproductive rate of fish stocks plays an important role in many aspects of fisheries science. A meta-analysis of available stock-recruitment datasets using the Ricker model has estimated these maximum annual reproductive rates to be within the 1-7 range for most species. However, this result may be a statistical artifact caused by the use of the Ricker model, which may be corrected by estimating these rates via semiparametric Bayesian models. In this study, we compared semiparametric and parametric analyses of 285 stock-recruitment datasets. The results showed that estimates of annual reproductive rates provided by the semiparametric Bayesian model are more dispersed than those based on the Ricker model. However, we also show that the estimates of annual reproductive rates provided by these two models are qualitatively similar. Because the semiparametric Bayesian model can provide good estimates of annual reproductive rate in various kinds of density dependence in the stock-recruitment relationship, we conclude that the Ricker model may be a reasonable approximation for estimating annual reproductive rates in empirical stock-recruitment datasets.

4-1. Introduction

Maximum reproductive rates play an important role in many aspects of conserving and managing fish populations (Myers 2001). In fisheries, maximum annual reproductive rates can be used for determining the upper limit to fishing mortality beyond which harvesting is unsustainable (Myers and Mertz 1998; Bravington et al. 2000; Cook 2000). From a conservation perspective, they can be used to assess the likelihood of a stock recovering from a depleted state and for designing recovery plans (Myers et al. 1997; Hutchings 2000). Despite their importance, previous estimates of maximum reproductive rate have been called into question. For example, Atlantic cod (*Gadus morhua*) stocks with positive population growth rates—obtained from calculations of maximum reproductive rate using the Ricker model (Myers et al. 1997) —do not show evidence of recovery 20+ years after a moratorium was implemented in 1992.

This suggests the possibility that the analyses of stock-recruitment (SR) data with the Ricker model may produce incorrect inferences of the maximum annual reproductive rate, α. In a meta-analysis of over 700 different stocks using the Ricker model, α was found to be within the 1-7 range in many species (Myers et al. 1999). However, it may be that α is better estimated with other parametric SR models such as the Beverton-Holt (BH), the sigmoid BH (SBH), or the Saila-Lorda (SL) models (Quinn and Deriso 1999; Liermann and Hilborn 2001; Needle 2002). Thus, it is important to identify the best estimate of α, and also its range among species. Selecting the best model via model selection criteria (e.g., Barrowman and Myers 2000) may not work because the 'correct' model is not always chosen over 'incorrect' models (Shelton and Healey 1999; see chapter 2), and different model selection criteria are inconsistent in selecting a single best model (Barrowman et al. 2003; Wang and Liu 2006; Zhou 2007; Ward 2008).

There are two approaches for resolving these statistical difficulties in inferring α. One approach is to use model averaging for producing a consensus estimate of α as a weighted average of model-specific estimates, where the weights are determined by the plausibility of the models (e.g., Brodziak and Legault 2005). In this way, it is possible to avoid the on-off nature of the model selection approach. Unfortunately, it is often the case that many models are equally plausible and averaging across the suite of estimates does not guarantee correction of bias in α.

The other, and probably better, approach is to abandon parametric forms entirely (e.g., Evans and Rice 1988; Bravington et al. 2000; see chapter 2). In chapter 2, we developed a semiparametric Bayesian (SB) model with a conditional Gaussian process (GP) model to obtain semiparametric estimates of α. Unlike previous nonparametric methods that require *ad hoc* and error-prone numerical calculation for estimating α (Evans and Rice 1988; Cook 1998; Cook 2000; Munch et al. 2005), the SB model developed in chapter 2 guarantees the direct interpretability of estimated α as the slope at the origin. Furthermore, unlike a previous nonparametric model designed to obtain inferences on α in compensatory SR relationships (Bravington et al. 2000), the SB model can also account for α in depensatory ones. Importantly, the SB model outperforms incorrect parametric models, and is nearly as good as the data-generating model, both in estimating α and in describing SR data (see chapter 2). Therefore, the SB model may be an ideal tool for obtaining unbiased estimates of α in empirical SR datasets where SR relationships are largely unknown.

It is therefore of interest to compare the SB and parametric estimates of α in empirical datasets and to examine the possibility that the generality in α across species is a statistical artifact. In this study, we compare SB estimates of $\ln\alpha$ with maximum likelihood estimates

(MLE) of lnα provided by the Ricker and the BH model in stock-recruitment datasets available from the 'Stock recruitment database' (http://www.mscs.dal.ca/~myers/welcome.html).

4-2. Methods

4-2-1. Datasets

We obtained all the SR datasets analyzed in this study from the 'Stock Recruitment database' (http://www.mscs.dal.ca/~myers/welcome.html). The database, as of 2011, has 788 SR datasets. The database provides information on taxonomy, sampling sites, methods for data collection, units for stock (usually weight, but number of individuals is used for salmonid species) and for recruitment (usually in number of individuals), and life history characteristics such as age at maturation, spawner biomass resulting from each recruit in the limit of zero fishing mortality ($SPR_{F=0}$), and natural mortality estimates (M).

We limited our analyses to datasets for which information on $SPR_{F=0}$ and M were available. This was done to allow for direct comparison with previous estimates of annual reproductive rate provided by the Ricker model (Myers et al. 1997; Myers et al. 1999). To maintain consistency with previous analyses, we multiplied raw data on recruitment by estimates of both $SPR_{F=0}$ and 1-exp(-M) before fitting models. Using adjusted recruitment enabled us to estimate the annual reproductive rate of stocks (Myers et al. 1997; Myers et a. 1999). Raw data on recruitment was multiplied only by $SPR_{F=0}$ in four semelparous salmon species, chum salmon (*Oncorhynchus keta*), pink salmon (*Oncorhynchus gorbuscha*), sockeye salmon (*Oncorhynchus nerka*), and chinook salmon (*Oncorhynchus tshawytscha*). This usually results in estimates of the biomass of spawners produced per each spawner over its lifetime (lifetime reproductive rate) in fish species (Myers et al. 1997; Myers et al. 1999). However, since reproduction is once-in-a-

lifetime event for the salmon species, annual reproductive rates and lifetime reproductive rates can be used interchangeably (Myers et al. 1997; Myers et al. 1999). Furthermore, we limited our analysis to datasets with over five years of paired stock and recruitment. The length of data varies from five years (sole, *Solea vulgaris*, identified as SOLEIIIa) to 74 years (whiting, *Merlangius merlangus*, identified as WHITNS2). After applying these data selection criteria, we obtained and analyzed 285 of the 788 SR datasets.

4-2-2. Estimation of annual reproductive rates

A general model for estimating annual reproductive rate, α, using SR data is given by:

$$R=S\exp[f(S)] \quad (1)$$

where S is spawning biomass and R is recruitment biomass adjusted for estimating α. The term $\exp[f(S)]$ describes the form of density dependence in this relationship; the specification of $f(S)$ will be described shortly. Since α is a tangent drawn to a SR function at S=0 (e.g., Myers et al. 1997; Myers et al. 1999; Myers et al. 2001), α can be obtained from the derivative of Eq. 1 with respect to S and evaluated at S=0. We therefore have $\alpha=\exp[f(0)]$, or equivalently

$$\ln\alpha= f(0). \quad (2)$$

Therefore, Eq. 2 indicates that $\ln\alpha$ can be interpreted as the intercept of a SR relationship when the SR relationship is represented in terms of recruits per spawner, i.e., in a variant of Eq. 1 with $y= f(S)$, where $y=\ln(R/S)$ (e.g., Myers et al. 1997; Myers et al. 1999; Myers et al. 2001).

The form of density dependence specified in $f(S)$ can affect the interpretation of α. When density dependence is compensatory, a monotonically decreasing function with S is used for $f(S)$, which guarantees $\ln\alpha$ to be the log of maximum annual reproductive rate. When it is depensatory, $f(S)$ is monotonically increasing at small values of S, with a global maximum at

some nonzero S, indicating that $\ln\alpha$ is merely the limiting annual reproductive rate as population density drops to zero (Liermann and Hilborn 2001; Courchamp et al. 2008).

In order to account for the two forms of density dependence using the same model, we used a conditional GP model for $f(S)$, with mean function $\mu(S)$ and covariance function $\Sigma(S,S')$:

$$f(S)\sim \mathrm{GP}[\mu(S), \Sigma(S,S')], \tag{3}$$

$$\mu(S)= \ln\alpha+\beta/S_{max},$$

$$\Sigma(S,S')=\tau^2\exp(-\varphi\ |S-S'|^2\ /S_{max}^2)-\tau^2\exp[-\varphi\ (S^2+S'^2)\ /S_{max}^2],$$

and obtained the estimate of annual reproductive rates under the SB framework (see chapter 2). The mean function in this GP model is linear with a parameter for the intercept, $\ln\alpha$, and a parameter that determines the strength of density dependence, β. This choice of mean function makes our prior guess for the shape of $f(S)$ to be similar to that of the Ricker model, but this guess can be easily overwhelmed by SR data that clearly show a different SR relationship (see chaper 2). The covariance function in this GP model is specified with a parameter determining the variance at a specific value of S, τ^2, and a parameter defining the smoothness of $f(S)$ over S, φ. Scaling by the maximum observed stock biomass, S_{max}, allows us to specify a generic prior for φ for all populations based on the expectation that reasonable SR models will have fewer than 2 turning points over the observed range of stock sizes (see chapter 2). This covariance function is non-stationary (i.e., the variance changes with S) and the variance is reduced to 0 at S =0. Therefore, with S=0, the viability in $f(0)$ is strictly determined by the posterior distribution for $\ln\alpha$, guaranteeing interpretability of estimated $\ln\alpha$ as annual reproductive rate (see chapter 2).

In fitting this model to SR data, we appended an error term ε to Eq. 1, $R=S\exp[f(S)+\varepsilon]$, to model R as an admixture of observation error and process uncertainty, where ε has a normal distribution with mean 0 and variance σ^2. We assumed S to be observed without error. The

inference for $\ln\alpha$, along with those for other parameters specifying the mean and covariance functions and the noise level in data σ^2, was obtained via MCMC (see chapter 2).

Myers et al. (1999) provided α values obtained from maximum likelihood estimates using the Ricker model. We therefore compared the posterior mode of the SB estimate of $\ln\alpha$ ($\ln\alpha_{SB}$) to MLE of $\ln\alpha$ obtained from parametric models. The parametric models were the stochastic Ricker ($R=\alpha S\exp(-\beta S+\varepsilon)$, where $\varepsilon\sim N(0,\sigma^2)$), for which the MLE of $\ln\alpha$ was calculated ($\ln\alpha_R$), and the stochastic Beverton-Holt ($R=\alpha S/(1+\gamma S)\exp(\varepsilon)$, where $\varepsilon\sim N(0,\sigma^2)$), for which the MLE of $\ln\alpha$ was estimated ($\ln\alpha_{BH}$).

4-3. Results

The SB model generated posterior distributions for $\ln\alpha$ on 264 of 285 SR datasets. In the remaining 21 data sets, the minimum observed stock size was too far from the origin to permit estimation of $\ln\alpha$. We restrict further attention to the 264 datasets for which estimates could be obtained.

To seek patterns in estimates of $\ln\alpha$ across the different models, we plotted the maximum likelihood estimates (MLE) of $\ln\alpha$ provided by the Ricker model ($\ln\alpha_R$) and the BH model ($\ln\alpha_{BH}$) against posterior modes of $\ln\alpha$ estimated with the SB model ($\ln\alpha_{SB}$) (Fig. 1). These figures show that, for most stocks, $\ln\alpha_R$ and $\ln\alpha_{SB}$ are similar (Fig. 1a), whereas estimates of $\ln\alpha_{BH}$ are much greater (Fig. 1b). Ranges for $\ln\alpha_R$ and $\ln\alpha_{SB}$ are also narrower than those for $\ln\alpha_{BH}$: -4 to 6 for $\ln\alpha_{SB}$ and $\ln\alpha_R$, while those for $\ln\alpha_{BH}$ are from -5 to 35. Recall that the values previously reported by Myers et al. (1999) were typically between 1 and 7. The percentage of stocks whose $\ln\alpha$ is within ln1 and ln7 is 64.77% in the SB analysis, 70.45% when using the Ricker model, and 2.65% when using the BH model (Table 1).

Analysis of these results on a species-by-species basis does not change the patterns observed in Fig. 1: $\ln\alpha_R$ and $\ln\alpha_{SB}$ are similar, and $\ln\alpha_{BH}$ is much greater than both (results not shown). However, the percentage of stocks whose $\ln\alpha$ is within ln1 and ln7 differ considerably across different species (Table 1). For example, there is a clear difference in range for $\ln\alpha_{SB}$ across four salmonids. The percentage of stocks whose $\ln\alpha$ is within ln1 and ln7 is 71.43% for chum salmon, 82.35% for pink salmon, 73.47% for sockeye salmon, and 42.86% for chinook salmon.

4-4. Discussion

The main finding in this paper is that estimates of $\ln\alpha$ provided by the SB model are more dispersed than those based on the Ricker model. This result indicates that, as Myers et al. (1999) were concerned, the generality in $\ln\alpha$ across stocks may be due to the usage of the Ricker model. However, we also show that estimates of $\ln\alpha$ provided by these two models (SB and Ricker) are still qualitatively similar. Because the SB model can provide good estimates of $\ln\alpha$ in both linear and nonlinear functions of $f(S)$ in the SR relationship (see chapter 2), we suggest that the Ricker model, although strictly linear in $f(S)$, is a reasonable approximation for empirical SR datasets. In contrast, we find that the estimates of $\ln\alpha$ provided by the BH model are unreasonably large in most SR datasets (as was previously shown by, e.g., Barrowman and Myers 2000), indicating that the BH model is not recommended for describing SR relationships at low stock levels.

We are aware that our analysis is not completely comparable to that of Myers et al. (1999). While we obtained estimates of $\ln\alpha$ assuming stocks are independent, Myers et al. (1999) considered meta-population structure in stocks of the same species and obtained estimates of $\ln\alpha$ using a hierarchical Ricker model. This generated species-specific estimates of $\ln\alpha$ as

well as stock-specific estimates of lnα, and they used the former to conclude that lnα for most species are within ln1 and ln7. In this study, we simply used this range as a benchmark against which to investigate the sensitivity of the choice of a model on stock-specific lnα. Therefore, for a SB analysis to be comparable to the previous analysis with the hierarchical Ricker model (Myers et al. 1999), the SB model used in this study has to be extended to obtain hierarchical estimates of lnα.

The SB estimation of lnα under meta-population modeling framework seems like a reasonable approach. In reality, fish populations cannot be easily identified as 'stocks', as chemical (e.g., Campana 1999) and genetic markers (e.g., Bohonak 1999) indicate that individuals move across different stocks. Moreover, spatial autocorrelation and shared environments among different stocks of a species (e.g., Caley et al. 1996) suggest similarity of life history characteristics across different stocks. Currently available models incorporating meta-population structure are limited to the use of parametric models (e.g., Myers et al. 1999; Myers et al. 2001; Chen and Holtby 2002; Barrowman et al. 2003; Michielsens and McAllister 2004; Gurney et al. 2010), with occasional incorporation of environmental variables (e.g., Dorn 2002; Forrest et al. 2010; Liermann et al. 2010). Therefore, more complex density dependence in the SR relationship is not accounted for. In light of this, a hierarchical SB model may be useful not only for examining the universality in lnα across species but also for better understanding the complex interactions of population structure with their respective environments.

From a statistical perspective, the use of meta-population modeling for the SR datasets would help obtain estimates of lnα in the 21 SR datasets for which the SB model was not able to generate reasonable posterior distributions of lnα. These datasets are short in length, highly

variable, and lacking in information at low stock sizes, all of which make it difficult for the SB model to generate inferences for lnα (see chapter 2). Meta-analysis may enable us to borrow information of different SR datasets to increase information for defining the SR relationships of the 21 SR datasets (Hilborn and Liermann 1998), whilst allowing for local variability in different stocks and avoiding fitting a model to noise (Stewart 2010).

Recently, a new database, 'RAM Legacy Stock Assessment Database' (http://ramlegacy.marinebiodiversity.ca/ram-legacy-stock-assessment-database) has updated the 'Stock recruitment database' to include information beyond 1995. In this study, we did not analyze SR datasets available from this newer database because some key information (e.g., $SPR_{F=0}$) was only given in a very limited number of datasets.

The results presented in this study have implications to management and conservation of fish stocks. Since lnα of a stock can be best estimated by the SB and Ricker models, the estimate of lnα can be considered as the best inference of the upper limit to harvest (Myers and Mertz 1998; Bravington et al. 2000; Cook 2000). Of course, harvesting below the upper limit does not always increase abundance of a fish stock (e.g., Atlantic cod stocks and Atlantic herring stocks), indicating that there remain a need for investigating other factors that may be delaying the rebuilding. For example, rebuilding of stocks may be halted by changes in species interactions (e.g., Walters and Kitchell, 2001) or by climate changes (e.g., Roessing et al. 2004), both of which can reduce recruitment.

In this study, we applied the SB model exclusively to fish stocks to compare the SB estimates of lnα with estimates of lnα provided by parametric models. The use of the SB model is applicable not only to fisheries problems, however, but also to more general ecological problems such as estimation of populations' growth rates. Like lnα, populations' growth rates

are also usually estimated by identifying the most appropriate form of density dependence in population dynamics. For example, Brook and Bradshaw (2006) and Gregory et al. (2010) estimated forms of density dependence in populations' time series, including both terrestrial and aquatic species available from the 'Global Population Dynamics Database' (http://www3.imperial.ac.uk/cpb/research/patternsandprocesses/gpdd). Importantly, they used parametric models, leaving open the possibility that growth rates and density dependence can be better approximated by other functional forms. Given the good performance of the SB model to correctly estimate lnα on simulated data (see chapter 2), a re-analysis of these datasets may be warranted.

4-5. Tables

Table 1. The frequency that estimated lnα is smaller than ln1, within ln1 and ln7, and greater than ln7 (in percentage). The results are based on the semiparametric Bayesian (SB) and parametric (Ricker, BH) analyses. N is the number of samples for each species.

Species	N	SB			Ricker			BH		
		lnα<ln1	ln1<lnα<ln7	lnα>ln7	lnα<ln1	ln1<lnα<ln7	lnα>ln7	lnα<ln1	ln1<lnα<ln7	lnα>ln7
Anadromous alewife (*Alosa pseudoharengus*)	5	0	40	60	0	80	20	0	40	60
Atlantic herring (*Clupea harengus*)	16	25	68.75	6.25	25	68.75	6.25	6.25	6.25	87.5
Atlantic cod (*Gadus morhua*)	24	12.5	62.5	25	16.67	66.67	16.67	0	0	100
Haddock (*Melanogrammus aeglefinus*)	11	9.09	90.91	0	9.09	90.91	0	0	0	100
Whiting (*Merlangius merlangus*)	6	0.33	0.5	0.17	0.33	0.5	0.17	0	0	100
Pollock or saithe (*Pollachius virens*)	5	20	80	0	0	100	0	0	0	100
Sole (*Solea vulgaris*)	5	40	40	20	20	60	20	0	0	100
Plaice (*Pleuronectes platessa*)	5	20	80	0	20	80	0	0	0	100
Chum salmon (*Oncorhynchus keta*)	7	0	71.43	28.57	0	71.43	28.57	0	0	100
Pink salmon (*Oncorhynchus gorbuscha*)	51	1.96	82.35	15.69	3.92	88.24	7.84	0	3.92	96.08
Sockeye salmon (*Oncorhynchus nerka*)	49	0	73.47	26.53	0	67.35	32.65	0	0	100
Chinook salmon (*Oncorhynchus tshawytscha*)	7	0	42.86	57.14	0	42.86	57.14	0	0	100
264 stocks (56 species) mixed	264	13.26	64.77	21.97	13.26	70.45	16.29	0.76	2.65	96.59

4-6. Figures

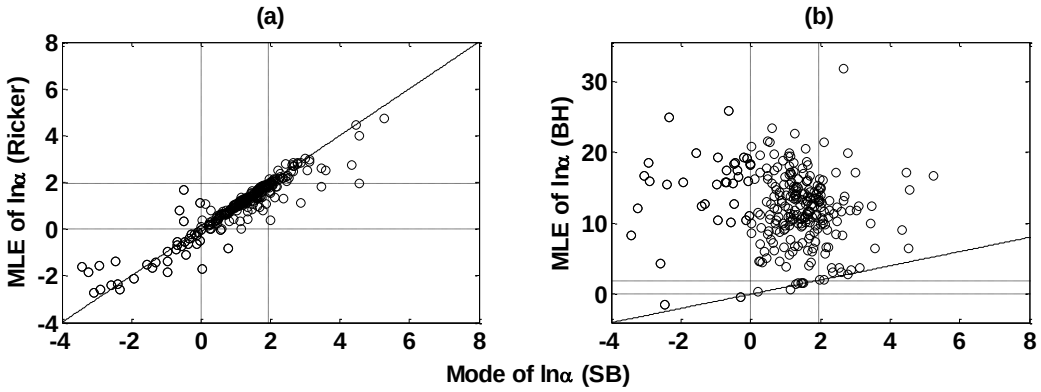

Figure 1. Comparison of the maximum likelihood estimates (MLE) of lnα (y axis) against modes of posterior distributions for lnα with the SB model (x axis) for 264 stocks. The vertical and horizontal lines indicate lnα to be ln1 and ln7 respectively. **a**: The Ricker model was used to obtain MLE for lnα. **b**: The BH model was used to obtain MLE for lnα.

Chapter 5

Allee effects may be more common than previously thought: a semiparametric assessment.

Key words

Allee effects, Allee effects threshold, depensation, quasi-extinction population size, semiparametric Bayesian modeling, Gaussian processes, stock-recruitment relationships

Abstract

Allee effects have long been recognized in theoretical studies of population dynamics, and hypothesized as potential contributors to population extinction. Although the necessary conditions for occurrence of Allee effects would seem to apply to many species (e.g., difficulty in finding mates at low density, mortality driven by generalist predators, etc.), evidence for Allee effects in biological populations is equivocal at best. We hypothesize that this apparent contradiction is due to insufficient power of previously used parametric models. We propose use of a semiparametric Bayesian model for improved detection of Allee effects. We test this hypothesis by comparing the frequency of Allee effects in fish populations estimated with parametric models to estimations from the semiparametric Bayesian model. Of 285 datasets analyzed, we found Allee effects in nine populations using the semiparametric Bayesian model, more than twice as many as were found in parametric models. These results suggest that Allee effects may be more common than previous studies have estimated.

5-1. Introduction

The reduction of per capita population growth at low population size is known as an Allee effect in honor of Dr. Warder Clyde Allee who first noted that small populations might fail because of difficulty finding mates at low densities, etc. (Courchamp et al. 2008). Allee effects are considered a primary driver of extinction (Boyce 1992; Dennis 2002; Morris and Doak 2002; Dulvy et al. 2004; Courchamp et al. 2008). To avoid extinction, populations must be maintained at sufficiently high densities to prevent Allee effects from dominating the dynamics (e.g., Grevstad 1999; Fischer and Lindenmayer 2000; Swain and Sinclair 2000; Walters and Kitchell 2001; Deredec and Courchamp 2007; Armstrong and Wittmer 2011). On the other hand, Allee effects can, in principle, be used to prevent harmful species invasions; by reducing the density of invading populations to the levels necessary for Allee effects to dominate population dynamics an invasion can be curtailed (e.g., Tayler and Hastings 2005; Tobin et al. 2011).

There is considerable evidence for 'component' Allee effects, i.e., Allee effects which are strongly tied to a reduced chance of conspecific presence at low population sizes (Stephens and Sutherland 1999). Increased difficulty in finding mates (e.g., Gascoigne et al. 2009), decreased cooperative defense against generalist predators (e.g., Gascoigne and Lipcius 2004), and decreased cooperative feeding (e.g., Grunbaum and Beit 2003) all occur at low population densities and can reduce individual fitness. Moreover, since decreased population size can reduce genetic heterogeneity, decreased fitness due to inbreeding depression can also occur (e.g., Willi et al. 2005). Furthermore, 'component' Allee effects can also occur when mortality by generalist predators to the small size classes increases, resulting in insufficient production of highly reproductive adults (Swain and Sinclair 2000; Walters and Kitchell 2001).

In light of their contributions to fitness, the existence of 'component' Allee effects found in many species (Berec et al. 2007; Kramer et al. 2009) suggests that Allee effects should also be apparent at the population level and detectable in population time series ('demographic' Allee effects, Stephens and Sutherland 1999). However, evidence for 'demographic' Allee effects (hereafter Allee effects) is equivocal at best. Previous analyses of time series data for terrestrial and aquatic populations (Saether et al. 1996; Sibly et al. 2005; Gregory et al. 2010) and commercially harvested fish populations (Myers et al. 1995; Liermann and Hilborn 1997; Chen et al. 2002; Barrowman et al. 2003; Nash et al. 2009) found limited evidence for Allee effects. Specifically, <1.2% of data sets in terrestrial and aquatic (Gregory et al. 2010) and <2.4% of data sets in commercially harvested fish populations (Myers et al. 1995) were found to exhibit Allee effects, leading to a general consensus that Allee effects are quite rare or hard to detect.

Some simulation studies have suggested that these results are due to insufficient statistical power of the parametric models for detecting Allee effects in typically short and highly variable ecological data (Shelton and Healey 1999; see chapter 3). That is, when data sets are short and noisy, the fit of parametric models incorporating Allee effects is not necessarily superior to analogous models without them (Sherton and Healey 1999; see chapter 3). Therefore, we hypothesize that the apparent rarity of demographic Allee effects is due in part to methodological shortcomings and that more powerful methods may reveal a greater prevalence of Allee effects. We test this hypothesis by comparing prevalence based on parametric models to that estimated from our recently developed semiparametric Bayesian approach using 285 datasets representing 56 species of commercially harvested fish populations.

5-2. Methods

5-2-1. Datasets

We compiled data on commercially harvested fish populations from the 'Stock Recruitment database' (http://www.mscs.dal.ca/~myers/welcome.html). The database, as of 2011, contains 788 datasets covering a wide range of taxa. Data are annotated with information regarding taxonomic details, data collection sites and sampling methods, adult weights (except for salmon species), number and weight of juveniles, and life history characteristics such as weight per individual for juveniles and natural mortality estimates.

For the SB analysis to be comparable to previous parametric analyses (Myers et al. 1995), we only analyzed the subset of cases for which (i) data on both adult biomass (A) and number of individuals for juveniles, and (ii) the adult biomass resulting from each juvenile were available. The original data on juveniles were multiplied by adult biomass resulting from each juvenile so that A and adjusted juvenile biomass (J) had the same units. This unit standardization enabled us to assess contribution of adult biomass to juvenile biomass production on a lifetime basis, making it possible to interpret the replacement line (i.e., $A=J$) as a benchmark against which to determine the presence of Allee effects. Based on these criteria, 285 datasets were used for analysis. The length of data ranged from 5 years (sole, *Solea vulgaris*, from the North Sea) to 74 years (whiting, *Merlangius merlangus*, from the North Sea). Unlike previous parametric analyses (Myers et al. 1995) that excluded datasets of less than 10 years, we included these for an additional15 datasets.

5-2-2. Allee effects detection

The relationship between adult biomass (A) and adjusted juvenile biomass produced (J) can be described by the model:

$$J=A\exp[f(A)+\varepsilon],\ \varepsilon\sim N(0,\sigma^2) \quad (1)$$

where $\exp[f(A)]$ models density dependence. Observation and process uncertainty is accounted for by ε, which is normally distributed with mean 0 and variance σ^2.

The form of density dependence is specified by the shape of $f(A)$ (Fig. E1 in Appendix E). If there is negative density dependence, $f(A)$ is a monotonically decreasing function with $f(A)>0$. If there are Allee effects, $f(A)$ near the origin is negative and increasing with A (Quinn and Deriso 1999; Liermann and Hilborn 2001; Needle 2002; Boukal and Berec 2002; Courchamp et al. 2008; see chapter 3). To be precise, the two conditions for Allee effects to be present are (i) $f(A)\leq 0$ and (ii) $f'(A)>0$ where $f'(A)\equiv df/dA$.

Unlike traditional approaches, which specify $f(A)$ with some parametric functions (e.g., Myers et al. 1995; Gregory et al. 2010), we modeled $f(A)$ with a Gaussian process (GP) model and inferred its form from data under a semiparametric Bayesian framework (see chapter 3). At a given adult mass, the inferred $f(A)$ and its derivative are bivariate normal, conditional on the GP hyperparameters. Therefore, we easily obtain the probability of the presence of Allee effects, $\Pr[f(A)\leq 0,\ f'(A)>0|\text{data}]$, by integration of a bivariate normal for $f(A)$ and $f'(A)$ given the parameters, followed by marginalization over distributions of the parameters. Because the presence of Allee effects is most relevant at small population sizes, we define an Allee effect index, π, as the probability evaluated at $A=0$ (Fig. E1 in Appendix E), i.e.,

$$\pi=\Pr[f(0)\leq 0, f'(0)>0|\text{data}]. \quad (2)$$

This inferred probability was compared to its prior probability, $\Pr[f(0)\leq 0, f'(0)>0]=0.25$ (see chapter 3), which provides a convenient benchmark against which to compare specific results. Thus, we ascertained the presence of Allee effects when data generated $\pi>0.25$. Details for implementing the SB model are given in chapter 3.

For the parametric assessment, we repeated the analysis of Myers et al. (1995) which used a likelihood ratio test to compare the fit of the sigmoid Beverton-Holt model [SBH, $J=\alpha A^{\gamma}/(1+\beta A)$] with that of the Beverton-Holt (BH) model [$J=\alpha A/(1+\beta A)$]. We refer to this likelihood ratio as LRT_{BH}. In addition, we compared performance of the Saila-Lorda model [SL, $J=\alpha A^{\gamma}\exp(-\beta A)$] with that of the Ricker model [$J=\alpha A\exp(-\beta A)$] (Quinn and Deriso 1999) and label this likelihood ratio LRT_R. In keeping with Myers et al. (1995), we used a χ^2 distribution with 1 degree of freedom and nominal confidence level of p=0.05, to test significance. Allee effects are deemed present when the maximum likelihood estimate of γ is greater than 1 and a likelihood test favors the SL or SBH models over the Ricker and the BH models respectively.

5-3. Results

The SB model generated posterior distributions for the probability of the presence of Allee effects, π, in 264 of 285 datasets; in 21 datasets π was not estimated because good estimates of π cannot be generated when data at low adult biomass are sparse (see chapter 3). Therefore, we analyzed the frequency of Allee effects based on the results of the 264 datasets. Supplementary figures show posterior inferences of $f(A)$ (Fig. E2 in Appendix E). A summary of assessments for the presence of Allee effects in the 264 data sets is given in Table E1 in Appendix E.

Comparison of the SB analysis with the parametric analyses showed that Allee effects were detected more often with the SB analysis than with the parametric analyses. The SB analysis detected Allee effects in 9 of 264 datasets (3.41%), whereas LRT_{Ricker} and LRT_{BH} detected them in 3 (1.14%) and 4 (1.52%) datasets, respectively (Table 1).

In the SB analysis, estimates of π and 95% credibility intervals showed that there is variation in the strength and uncertainty of evidence for Allee effects across the populations (Table 2, Fig. 1). Among the nine populations found to exhibit Allee effects, the strongest evidence for Allee effects was found in the Atlantic cod population from The Newfoundland (Canada), with π=0.92. The very narrow confidence intervals of π for this population indicated that the uncertainty level in the assessment is the lowest of the nine populations. The narrowest evidence for Allee effects among the nine populations was found in the bigeye tuna population of the West Atlantic, with π=0.32. The population with the most ambiguous evidence of Allee effects was pink salmon of Burke, British Columbia (Canada). π for this population was 0.68 but the confidence intervals were the widest of the nine populations.

The probabilities of Allee effect presence for these nine populations were calculated over entire range of adult biomass (*A*) (Fig. 2). There were ranges of *A* in which the probabilities were close to 1, and the probabilities were monotonically decreasing over *A* (Fig. 2). Of the nine populations, Atlantic herring (Iceland spring spawner) (Fig. 2b), Atlantic cod (The Newfound land, Canada) (Fig. 2c), bluefish (East Coast, USA) (Fig. 2e), and bigeye tuna (West Atlantic) (Fig. 2f), all displayed clear Allee effects. The other five populations (Atlantic herring (Georges bank), whiting (North Sea), red porgy (Atlantic ocean off North Carolina), sablefish (West Coast, USA), pink salmon (Burke, B.C., Canada)) also exhibited Allee effects, but the evidence was weaker.

With the exception of a population of Atlantic herring (Iceland spring spawner), Allee effects were not detected in any population consistently with all three methods (the SB analysis, LRT_{Ricker}, LRT_{BH}) (Table 2). Although the SB analysis and LRT_{BH} detected Allee effects in a population of Atlantic herring (Georges bank), LRT_{Ricker} did not. Similarly, the SB analysis and LRT_{Ricker} detected Allee effects in a population of Atlantic cod (The Newfoundland, Canada) but LRT_{BH} did not. In addition to these three populations, the SB analysis uniquely detected Allee effects in six other populations: whiting (North Sea), bluefish (East Coast, USA), bigeye tuna (West Atlantic), red porgy (Atlantic ocean off North Carolina), sablefish (West Coast, USA), and pink salmon (Burke, B.C., Canada). In contrast, there were three populations in which only parametric analyses detected Allee effects: a pink salmon population from Utka river (Kamchatka, Russia) with LRT_{Ricker}, and a pink salmon population from Kitimat (B.C., Canada) and a sockeye salmon population from Adams Complex (B.C., Canada) with LRT_{BH}.

5-4. Discussion

In this study, we showed that the SB analysis detected Allee effects in fish populations more than twice as often as the parametric analyses (Table 1). These results support our hypothesis that insufficient power of parametric models to correctly detect Allee effects (Shelton and Healey 1999; see chapter 3) may contribute to their apparent scarcity among fish populations (Myers et al. 1995; Liermann and Hilborn 1997; Barrowman et al. 2003).

Despite the fact that we detected twice as many populations with Allee effects, demographic Allee effects still appear to be quite rare. Either this apparent rarity is a statistical artifact or demographic Allee effects don't emerge except in highly idealized circumstances. The prevalence of Allee effects in fish populations is still ambiguous due to insufficient data; for 9 of the 12 populations demonstrating Allee effects, the uncertainty level in π was quite large.

Except for two Pink salmon populations (Kitimat of B.C. in Canada N=11 and Utka river of Kamchatka in Russia N=10) whose short time series clearly exhibit no Allee effects (Fig. 1, Fig. E1 in Appendix E, and Table 2), the uncertainty in π is inversely related to sample size (Table 2).

Moreover, the inferred rarity of Allee effects in fish populations may be due to oversimplification to the models we used. At present, our model treats all unexplained variation as noise, ignoring environmental effects and assumes no migration. Although our semiparametric model can readily include environmental covariates (e.g., Chen and Ware 1999; Chen et al. 2000; Chen and Irvine 2001; Wang et al. 2009), we have not yet extended our Allee effect index to address environmental effects. However, mechanisms connecting environmental drivers to Allee effects are not clear and Gregory et al. (2010) found minimal gain in ability to detect Allee effects when environmental variable were included.

Reassessment with models accounting for migration may change the estimated prevalence of Allee effects. However, Allee effects detected using models with migration may be irrelevant to extinction risk of marine populations. A simulation study using a model with Allee effects and migration showed a greater chance of persistence in populations with migration than without (Brassil 2001). Given the empirical evidence indicating the commonness of migration in marine populations (e.g., Campana 1999), marine populations may be more resistant to extinction via Allee effects than terrestrial ones are.

That said, it may well be that demographic Allee effects are rare in marine fish populations. Demographic Allee effects occur only when component Allee effects are present (Courchamp et al. 2008), but traits common in marine fishes are likely to dampen Allee effects. For example, schooling behavior, pervasively found in marine fishes (e.g., herring, sprat, cod) (Froese and Pauly 2012), may facilitate finding mates even at very low densities (e.g., Gascoigne

et al. 2009). Schooling also enhances the effectiveness of cooperative defense against generalist predators (e.g., Gascoigne and Lipcius 2004). Moreover, typical forms of predation by marine fishes (e.g., filter feeding, opportunistic feeding) (Froese and Pauly 2012) do not require cooperation with conspecifics. Furthermore, migration reduces the chance of inbreeding depression to occur (Campana 1999).

Even if some traits of marine fishes cause component Allee effects, complex interactions among different traits may dampen or prevent demographic Allee effects (Stephens et al. 1999; Courchamp et al. 2008; Mieszkowska et al. 2009). For example, temporal benefits of conspecifics with increasing population density at the low level may be offset by reduced resource availability for an individual. Finally, although size-selective harvest is hypothesized as a driver for component Allee effects (e.g., Atlantic cod (*Gadus morhua*)) (Walter and Kitchell 2001; Rowe et al. 2004), to our knowledge no study has been conducted to rigorously examine the link between size-selective harvest and component Allee effects among marine fishes.

In this study, we applied the SB model exclusively to fish populations, making a direct comparison of the SB and parametric assessments (Myers et al. 1995). However, the use of the SB model is applicable to any population time series. Given the high performance of the SB model for correct detection of the presence of Allee effects on simulated data (see chapter 3), we suggest that re-analysis of datasets analyzed in previous studies, including those on terrestrial species (Sibly et al. 2005; Gregory et al. 2010), may be warranted.

5-5. Tables

Table 1. The frequency of Allee effects in 264 fish populations determined with the SB analysis and the parametric analyses (LRT_{Ricker} and LRT_{BH}). The frequency is compared with that determined in Myers et al. (1995).

	Total	SB analysis	LRT_{Ricker}	LRT_{BH}
Myers et al. 1995	**129**	**N/A**	**N/A**	**2.33% (3/129)**
This study	**264**	**3.41% (9/264)**	**1.14% (3/264)**	**1.52% (4/264)**

Table 2. Assessment for the presence of Allee effects using the SB model (π) and parametric models (LRT_{Ricker} and LRT_{BH}) for 12 populations. N is sample size of population data. Symbols (Y and N) for LRT_{Ricker} and LRT_{BH} indicate populations with Allee effects [Y] and without Allee effects [N]. Var(π) is the variance of π. π written with a bold font indicates populations with Allee effects.

Genus, species **(common name)**	**Sampling sites**	**N**	**LRT(R)**	**LRT(BH)**	π	**Var(π)**
Clupea harengus **(Herring)**	**Georges bank**	15	N	**Y**	**0.68**	**0.06**
	Iceland (spring spawner)	23	**Y**	**Y**	**0.67**	**0.04**
Gadus morhua **(Cod)**	**The Newfound land, Canada**	27	**Y**	N	**0.92**	**0.02**
Merlangius merlangus **(Whiting)**	**North Sea**	74	N	N	**0.84**	**0.03**
Pomatomus saltatrix **(Bluefish)**	**East Coast, USA**	14	N	N	**0.52**	**0.07**
Thunnus obesus **(Bigeye Tuna)**	**West Atlantic**	35	N	N	**0.32**	**0.07**
Pagrus pagrus **(Red porgy)**	**Atlantic ocean off North Carolina**	20	N	N	**0.87**	**0.04**
Anoplopoma fimbria **(Sablefish)**	**West Coast, USA**	18	N	N	**0.47**	**0.08**
Oncorhynchus gorbuscha **(Pink salmon)**	**Burke, B.C., Canada**	11	N	N	**0.68**	**0.09**
	Kitimat, B.C., Canada	11	N	**Y**	0.00	0.00
	Utka river, Kamchatka, Russia	10	**Y**	N	0.00	0.00
Oncorhynchus nerka **(Sockeye salmon)**	**Adams Complex, B.C., Canada**	39	N	**Y**	0.00	0.00

5-6. Figures

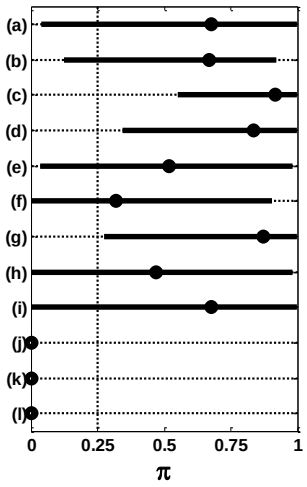

Figure 1. The probability of the presence of Allee effects, π [dot], and its 95% confidence intervals [solid] for 12 populations: (a) Atlantic herring (Georges bank), (b) Atlantic herring (Iceland spring spawner), (c) Atlantic cod (The Newfound land, Canada), (d) whiting (North Sea), (e) bluefish (East Coast, USA), (f) bigeye tuna (West Atlantic), (g) red porgy (Atlantic ocean off North Carolina), (h) sablefish (West Coast, USA), (i) pink salmon (Burke, B.C., Canada), (j) pink salmon (Kitimat, B.C., Canada), (k) pink salmon (Utka river, Kamchatka, Russia), and (l) sockeye salmon (Adams Complex, B.C., Canada). The vertical dotted line indicates prior probability of the presence of Allee effects (0.25).

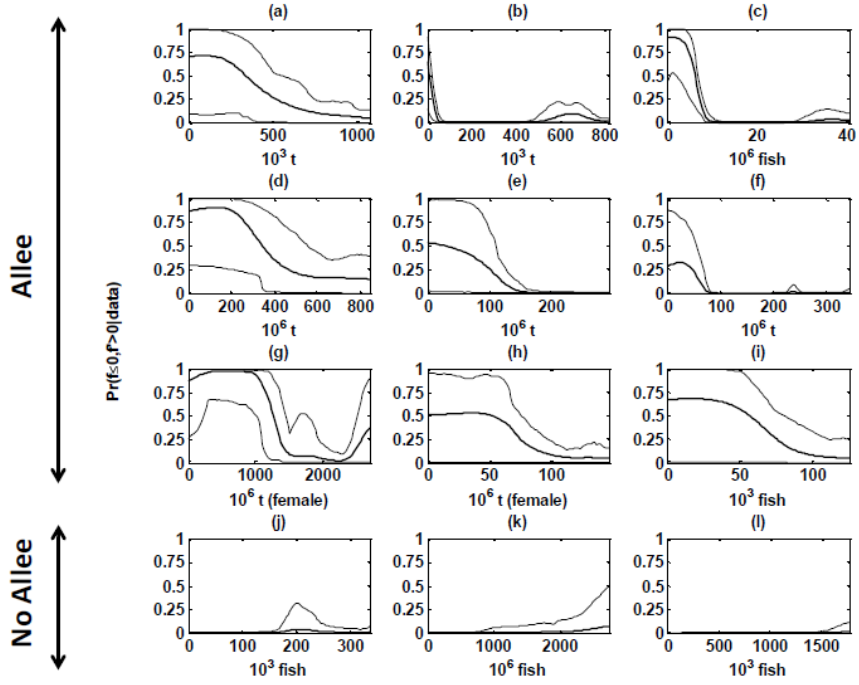

Figure 2. The posterior probability for the presence of Allee effects for 12 populations which exhibit Allee effects. 'Allee' indicates populations which the SB model detected Allee effects (a-i). 'No Allee' indicates populations which only parametric models detected Allee effects (j-l). We plotted the mean of the posterior probability [thick solid line] and the 95% confidence intervals of the posterior probability [thin solid line]. Note that scales in x axis differs across different populations. (a) Atlantic herring (Georges bank), (b) Atlantic herring (Iceland spring spawner), (c) Atlantic cod (The Newfound land, Canada), (d) whiting (North Sea), (e) bluefish (East Coast, USA), (f) bigeye tuna (West Atlantic), (g) red porgy (Atlantic ocean off North Carolina), (h) sablefish (West Coast, USA), (i) pink salmon (Burke, B.C., Canada), (j) pink salmon (Kitimat, B.C., Canada), (k) pink salmon (Utka river, Kamchatka, Russia), (l) sockeye salmon (Adams Complex, B.C., Canada).

Literature cited

Armstrong, D.P., and Wittmer, H.U. 2011. Incorporating Allee effects into reintroduction strategies. *Ecological Research*. 26(4): 687-695.

Barrowman, N.J. and Myers, R.A. 2000. Still more spawner–recruitment curves: the hockey stick and its generalizations. *Canadian Journal of Fisheries and Aquatic Sciences*. 57: 665–676.

Barrowman, N.J., Myers, R.A., Hilborn, R., Kehler, D.G., and Field, C.A. 2003. The Variability among Populations of Coho Salmon in the Maximum Reproductive Rate and Depensation. *Ecological Applications*. 13(3): 784-793.

Bence, J.R. 1995. Analysis of Short Time Series: Correcting for Autocorrelation. *Ecology*. 76(2): 628-639.

Berec, L., Angulo, E., and Courchamp, F. 2007. Multiple Allee effects and population management. *Trends in Ecology and Evolution*. 22(4): 185-191.

Berger, J.O. 1985. *Statistical Decision Theory and Bayesian Analysis (Springer Series in Statistics)*. Springer.

Bohonak, A.J. 1999. Dispersal, gene flow, and population structure. *The Quarterly Review of Biology*. 74(1): 21-45.

Boukal, D.S., and Berec, L. 2002. Single-species Models of the Allee Effect: Extinction Boundaries, Sex Ratios and Mate Encounters. *Journal of Theoretical Biology*. 219(3): 375-394.

Boyce, M.S. 1992. Population viability analysis. *Annual Review of Ecology and Systematics*. 23: 481-506.

Brassil, C.E. 2001. Mean time to extinction of a metapopulation with an Allee effect. *Ecological Modelling*. 143(1-2): 9-16.

Bravington, M.V., Stokes, T.K., and O'Brien, C.M. 2000. Sustainable recruitment: the bottom line. *Marine Freshwater Research*.51: 465–75.

Brodziak, J. and Legault, C.M. 2005. Model averaging to estimate rebuilding targets for overfished stocks. *Canadian Journal of Fisheries and Aquatic Sciences*. 62: 544–562.

Brook, B.W., and Bradshaw, C.J.A. 2006. Strength of Evidence for Density Dependence in Abundance Time Series of 1198 Species. *Ecology*. 87(6): 1445-1451.

Caley, M.J., Carr, M.H., Hixon, M.A., Hughes, T.P, Jones, G.P., and Menge, B.A. 1996. Recruitment and the local dynamics of open marine populations. *Annual Review of Ecology and Systematics*. 27: 477–500.

Campana, S.E. 1999. Chemistry and composition of fish otoliths: pathways, mechanisms and applications. *Marine Ecology Progress Series*. 188: 263-297.

Chen, D.G., and Ware, D.M. 1999. A neural network model for forecasting fish stock recruitment. *Canadian Journal of Fisheries and Aquatic Sciences*. 56: 2385–2396.

Chen, D.G., Hargreaves, N.B., Ware, D.M., and Liu, Y. 2000. A fuzzy logic model with genetic algorithm for analyzing fish stock–recruitment relationships. *Canadian Journal of Fisheries and Aquatic Sciences*. 57: 1878–1887.

Chen, D.G., and Irvine, J.R. 2001. A semiparametric model to examine stock–recruitment relationships incorporating environmental data. *Canadian Journal of Fisheries and Aquatic Sciences.* 58*:* 1178–1186.

Chen, D.G. and Holtby, L.B. 2002. A regional meta-model for stock-recruitment analysis using an empirical Bayesian approach. *Canadian Journal of Fisheries and Aquatic Sciences*. 59(9): 1503-1514.

Chen, D.G., Irvine, J.R., and Cass, A.J. 2002. Incorporating Allee effects in fish stock-recruitment models and applications for determining reference points. *Canadian Journal of Fisheries and Aquatic Sciences*. 59: 242–249.

Cook, R.M. 1998. A sustainability criterion for the exploitation of North Sea cod. *ICES Journal of Marine Science*. 55: 1061–1070.

Cook, R. 2000. A rough guide to population change in exploited fish stocks. *Ecology Letters*. 3: 394-398.

Courchamp, F., Clutton-Brock, T., and Grenfell, B. 1999. Inverse density dependence and the Allee effect. *Trends in Ecology and Evolution*. 14(10): 405-410.

Courchamp, F., Berec, L., and Gascoigne, J. 2008. *Allee Effects in Ecology and Conservation*. Oxford University Press (USA).

Dennis, B. 2002. Allee effects in stochastic populations. *Oikos*. 96(3): 389–401.

Deredec, A., and Courchamp, F. 2007. Importance of the Allee effect for reintroductions. *Ecoscience*. 14(4): 440-451.

Dietz, T., Ostrom, E., and Stern, P.C. 2003. The Struggle to Govern the Commons. *Science*. 302(5652): 1907-1912.

Dorn, M.W. 2002. Advice on West Coast rockfish harvest rates from Bayesian meta-analysis of stock-recruit relationships. *North American Journal of Fisheries Management*. 22(1): 280-300.

Dulvy, N.K., Ellis, J.R., Goodwin, N.B., Grant, A., Reynolds, J.D., and Jennings, A. 2004. Methods of assessing extinction risk in marine fishes. *Fish and Fisheries*. 5: 255–276

Evans, G.T., and Rice, J.C. 1988. Predicting recruitment from stock size without the mediation of a functional relation. *Journal du Conseil: ICES Journal of Marine Science*. 44: 111-122.

Fenichel, E.P., Tsao, J.I., Jones, M.L., and Hickling, G.J. 2008. Real options for precautionary fisheries management. *Fish and Fisheries*. 9: 121–137.

Fischer, J., and Lindenmayer, D.B. 2000. An assessment of the published results of animal relocations. *Biological Conservation*. 96: 1-11.

Forrest, R.E., McAllister, M.K., Dorn, M.W., Martell, S.J.D., and Stanley, R.D. 2010. Hierarchical Bayesian estimation of recruitment parameters and reference points for Pacific rockfishes (Sebastes spp.) under alternative assumptions about the stock-recruit function. *Canadian Journal of Fisheries and Aquatic Sciences*. 67(10): 1611-1634.

Francis, R.I.C.C., and Shotton, R. 1997. "Risk" in fisheries management: a review. *Canadian Journal of Fisheries and Aquatic Sciences*. 54: 1699-1715.

Froese, R. and Pauly, D. Editors. 2012. FishBase. World Wide Web electronic publication. www.fishbase.org, version (02/2012).

Gascoigne, J.C., and Lipcius, R.N. 2004. Allee effects driven by predation. *Journal of Applied Ecology*. 41: 801–810.

Gascoigne, J., Berec, L., Gregory, S., and Courchamp, F. 2009. Dangerously few liaisons: a review of mate-finding Allee effects. *Population Ecology*. 51: 355-372.

Gelman, A., Carlin, J.B., Stern, H.S., and Rubin, D.B. 2003. *Bayesian Data Analysis* (2nd edition). Chapman and Hall/CRC press.

Global Population Dynamics Database. http://www3.imperial.ac.uk/cpb/research/patternsandprocesses/gpdd.

Gregory, S.D., Bradshaw, C.J.A., Brook, B.W., and Courchamp, F. 2010. Limited evidence for the demographic Allee effect from numerous species across taxa. *Ecology*. 91(7): 2151-2161.

Grevstad, F.S. 1999. Experimental invasions using biological control introductions: the influence of release size on the chance of population establishment. *Biological Invasions*. 1(4): 313-323.

Grunbaum, D. and Veit, R.R. 2003. Black-browed albatrosses foraging on Antarctic krill: density-dependence through local enhancement? *Ecology*. 84: 3265–3275.

Gurney, W.S.C., Bacon, P.J., McKenzie, E., McGinnity, P., Mclean, J., Smith, G., and Youngson, A. 2010. Form and uncertainty in stock-recruitment relations: observations and implications for Atlantic salmon (*Salmo salar*) management. *Canadian Journal of Fisheries and Aquatic Sciences*. 67(6): 1040-1055.

He, X., Mangel, M., and MacCall, A. 2006. A prior for steepness in stock-recruitment relationships, based on an evolutionary persistence principle. *Fisheries Bulletin*. 104: 428-433.

Hilborn, R. and Walters, C.J. 1992. *Quantitative Fisheries Stock Assessment: Choice, Dynamics and Uncertainty*. Chapman and Hall, New York.

Hilborn, R., and Liermann, M. 1998. Standing on the shoulders of giants: learning from experience in fisheries. *Reviews in Fish Biology and Fisheries*. 8(3): 273-283.

Hilborn, R., Maguire, J. J., Parma, A.M., and Rosenberg, A. 2001. The Precautionary Approach and risk management: can they increase the probability of successes in fishery management? *Canadian Journal of Fisheries and Aquatic Sciences*. 58: 99-107.

Hill, S.L., Watters, G.M., Punt, A.E., McAllister, M.K., Quere, C.L., and Turner, J. 2007. Model uncertainty in the ecosystem approach to fisheries. *Fish and Fisheries*. 8: 315–336.

Hogg, R.V., McKean, J.W. and Craig, A. 2004. *Introduction to Mathematical Statistics* (6th edition). Prentice Hall.

Hutchings, J.A. 2000. Collapse and recovery of marine fishes. *Nature*. 406: 882-885.

Kehler, D.G., Myers, R.A., Field, C.A. 2002. Measurement error and bias in the maximum reproductive rate for the Ricker model. 59(5): 854-864.

Kramer, A.M., Dennis, B., Liebhold, A.M., and Drake, J.M. 2009. The evidence for Allee effects. *Population Ecology*. 51: 341-354.

Lande, R., Engen, S., and Saether, B.E. 1994. Optimal harvesting, economic discounting and extinction risk in fluctuating populations. *Nature*. 372: 88 – 90.

Liermann, M., and Hilborn, R. 1997. Depensation in fish stocks: a hierarchical Bayesian meta-analysis. *Canadian Journal of Fisheries and Aquatic Sciences*. 54: 1976–1984.

Liermann, M. and Hilborn, R.. 2001. Depensation: evidence, models and implications. *Fish and Fisheries*. 2: 33-58.

Liermann, M.C., Sharma, R., and Parken, C.K. 2010. Using accessible watershed size to predict management parameters for Chinook salmon, *Oncorhynchus tshawytscha*, populations with little or no spawner-recruit data: a Bayesian hierarchical modelling approach. *Fisheries Management and Ecology*. 17(1): 40-51.

Ludwig, D., Hilborn, R., and Waters, C. 1993. Uncertainty, Resource Exploitation, and Conservation: Lessons from History. *Science*. 260(5104): 17+36.

Michielsens, C.G.J., and McAllister, M.K. 2004. A Bayesian hierarchical analysis of stock–recruit data: quantifying structural and parameter uncertainties. *Canadian Journal of Fisheries and Aquatic Sciences*. 61: 1032–1047.

Mieszkowska, N., Genner, M.J., Hawkins, S.J., and Sims, D.W. 2009. Effects of Climate Change and Commercial Fishing on Atlantic Cod. *Gadus morhua*. *Advances in Marine Biology*. 56: 213-273.

Millar, R.B. 2002. Reference priors for Bayesian fisheries models. *Canadian Journal of Fisheries and Aquatic Sciences*. 59: 1492–1502.

Morris, W.F., and Doak, D.F. 2002. *Quantitative Conservation Biology: Theory and Practice of Population Viability Analysis*. Sinauer Associates.

Munch, S.B., Kottas, A. and Mangel, M. 2005. Bayesian nonparametric analysis of stock-recruitment relationships. *Canadian Journal of Fisheries and Aquatic Sciences*. 62: 1808-1821.

Myers, R.A. 2001. Stock and recruitment: generalizations about maximum reproductive rate, density dependence, and variability using meta-analytic approaches. *ICES Journal of Marine Science*. 58: 937-951.

Myers, R.A., Rosenberg, A.A., Mace, P.M., Barrowman, N., and Restrepo, V.R. 1994. In search of thresholds for recruitment overfishing. *ICES Journal of Marine Science*. 51: 191-205.

Myers, R.A., and Barrowman, N.J. 1995. Time series bias in the estimation of density-dependent mortality in stock-recruitment models. *Canadian Journal of Fisheries and Aquatic Sciences*. 52: 223–232.

Myers, R.A., Barrowman, N.J., Hutchings, J.A., and Rosenberg, A.A. 1995. Population dynamics of exploited fish stocks at low population levels. *Science*. 269: 1106–1108.

Myers, R.A., and Mertz, G. 1997. Maximum population growth rates and recovery times for Atlantic cod, *Gadus morhua*. *Fisheries Bulletin*. 95: 762-772.

Myers, R.A., and Mertz, G. 1998. The limits of exploitation: A precautionary approach. *Ecological Applications*. 8(1) Supplement: S165–S169.

Myers, R.A., Bowen, K.G., and Barrowman, N.J. 1999. Maximum reproductive rate of fish at low population sizes. *Canadian Journal of Fisheries and Aquatic Sciences*. 56: 2404-2419.

Myers, R.A., MacKenzie, B.R., Bowen, K.G., and Barrowman, N.J. 2001. What is the carrying capacity for fish in the ocean? A meta-analysis of population dynamics of North Atlantic cod. *Canadian Journal of Fisheries and Aquatic Sciences*. 58: 1464–1476.

Nash, R.D.M., Dickey-Collas, M., and Kell, L.T. 2009. Stock and recruitment in North Sea herring (*Clupea harengus*); compensation and depensation in the population dynamics. *Fisheries Research*. 95: 88-97.

Needle, C.L. 2002. Recruitment models: diagnosis and prognosis. *Reviews in Fish Biology and Fisheries.* 11: 95–111.

O'Hagan, A., and Kingman, J.F.C. 1978. Curve Fitting and Optimal Design for Prediction. *Journal of the Royal Statistical Society.Series B (Methodological)*. 40(1): 1-42.

Ostrom, E., Burger, J., Field, C.B., Norgaard, R.B., and Policansky, D. 1999. Revisiting the Commons: Local Lessons, Global Challenges. *Science*. 284(5412): 278-282.

Punt, A. E., and Hilborn, R. 1997. Fisheries stock assessment and decision analysis: the Bayesian approach. *Reviews in Fish Biology and Fisheries*. 7: 35-63.

Pyper, B.J., and Peterman, R.M. 1998. Comparison of methods to account for autocorrelation in correlation analyses of fish data. *Canadian Journal of Fisheries and Aquatic Sciences*. 55: 2127–2140.

Quinn, T.J., and Deriso, R.B. 1999. *Quantitative Fish Dynamics*. Oxford University Press (USA).

RAM Legacy Stock Assessment Database. http://ramlegacy.marinebiodiversity.ca/ram-legacy-stock-assessment-database.

Rasmussen, C.E. and Williams C.K.I. 2006. *Gaussian Processes for Machine Learning*. The MIT Press.

Roessig, J.M., Woodley, C.M., Cech, J.J.Jr. and Hansen, L.J. 2004. Effects of global climate change on marine and estuarine fishes and fisheries. *Reviews in Fish Biology and Fisheries*. 14: 251–275.

Rowe, S., Hutchings, J.A., Bekkevold, D., and Rakitin, A. 2004. Depensation, probability of fertilization, and the mating system of Atlantic cod (*Gadus morhua*). *ICES Journal of Marine Science*. 61(7): 1144-1150.

Saether, B.E., Ringsby, T.H., and Roskaft, E. 1996. Life history variation, population processes and priorities in species conservation: towards a reunion of research paradigms. *Oikos*. 77:217-226.

Saila, S.B., Recksiek, C.W., and Prager, M.H. 1988. *Basic fishery science programs: a compendium of microcomputer programs and manual of operation*. Elsevier Science (USA).

Shelton, P.A., and Healey, B.P. 1999. Should depensation be dismissed as a possible explanation for the lack of recovery of the northern cod (*Gadus morhua*) stock? *Canadian Journal of Fisheries and Aquatic Sciences*. 56: 1521-1524.

Sibly, R.M., Barker, D., Denham, M.C., Hone, J. and Pagel, M. 2005. On the Regulation of Populations of Mammals, Birds, Fish, and Insects. *Science*. 209: 607-610.

Stephens, P.A., and Sutherland, W.J. 1999. Consequences of the Allee effect for behaviour, ecology and conservation. *Trends in Ecology and Evolution*. 14(10): 401-405.

Stephens, P.A., Sutherland, W.J., and Freckleton, R.P. 1999. What is the Allee effect? *Oikos*. 87(1): 185-190.

Stewart, G. 2010. Meta-analysis in applied ecology. *Biology Letters*. 6: 78-81.

Stock Recruitment Database. http://www.mscs.dal.ca/~myers/welcome.html.

Swain, D.P., and Sinclair, A.F. 2000. Pelagic fishes and the cod recruitment dilemma in the Northwest Atlantic. *Canadian Journal of Fisheries and Aquatic Sciences*. 57: 1321–1325.

Taylor, C.M., and Hastings, A. 2005. Allee effects in biological invasions. *Ecology Letters*. 8: 895-908.

Tobin, P.C., Berec, L., and Liebhold, A.M. 2011. Exploiting Allee effects for managing biological invasions. *Ecology Letters*. 14: 615–624.

Turchin, P. 2003. *Complex population dynamics: a theoretical/empirical synthesis*. Princeton University Press.

Wade, P.R. 2000. Bayesian Methods in Conservation Biology. *Conservation Biology*. 14(5): 1308-1316.

Walters, C.J. 1990. A Partial Bias Correction Factor for Stock–Recruitment Parameter Estimation in the Presence of Autocorrelated Environmental Effects. *Canadian Journal of Fisheries and Aquatic Sciences*. 47: 516–519.

Walters, C., and Kitchell, J.F. 2001. Cultivation/depensation effects on juvenile survival and recruitment: implications for the theory of fishing. *Canadian Journal of Fisheries and Aquatic Sciences*. 58: 39–50.

Wang, Y. and Liu, Q. 2006. Comparison of Akaike information criterion (AIC) and Bayesian information criterion (BIC) in selection of stock–recruitment relationships. *Fisheries Research*. 77: 220-225.

Wang, S., Morishima, G., Sharma, R., and Gilbertson, L. 2009. The Use of Generalized Additive Models for Forecasting the Abundance of Queets River Coho Salmon. *North American Journal of Fisheries Management*. 29: 423–433.

Ward, E.J. 2008. A review and comparison of four commonly used Bayesian and maximum likelihood model selection tools. *Ecological Modelling*. 211(1-2): 1-10.

Willi,Y., van Buskirk, J., and Fischer, M. 2005. A Threefold Genetic Allee Effect: Population Size Affects Cross-Compatibility, Inbreeding Depression and Drift Load in the Self-Incompatible *Ranunculus reptans*. *Genetics*. 169: 2255–2265.

Wood, S.N., and Thomas, M.B. 1999. Super-sensitivity to structure in biological models. *Proceedings of the Royal Society of London Series B-Biological Sciences*. 266: 565-570.

Ylvisaker, N. D. 1965. The expected number of zeros of a stationary Gaussian process. *The Annals of Mathematical Statistics*. 36: 1043-1046.

Zhou, S. 2007. Discriminating alternative stock–recruitment models and evaluating uncertainty in model structure. *Fisheries Research*. 86: 268–279.

Appendices

Appendix A: The conditional Gaussian process prior (chapter 2)

The conditional GP prior $f(S)$ can be derived first by applying the techniques for obtaining the conditional normal distribution from a joint normal distribution. In the standard multivariate normal setting, when x_1 and x_2 are jointly normal with mean $[\mu_1, \mu_2]^T$ and covariance Σ, the distribution for x_2 given x_1 is

$$\mu_{2|1} = \mu_2 + \Sigma_{2,1}\left(\Sigma_{1,1}\right)^{-1}(x_1 - \mu_1) \tag{A1}$$

$$\Sigma_{2|1} = \Sigma_2 - \Sigma_{2,1}\left(\Sigma_{1,1}\right)^{-1}{\Sigma_{2,1}}^T,$$

where $\Sigma_{i,j}$ denotes the partition of Σ corresponding covariance among i and j, e.g., $\Sigma_{1,2}$, represents the covariances among elements of vectors x_1 and x_2 (e.g., Hogg et al. 2004).

To make use of this we construct a joint GP prior:

$$\begin{bmatrix} f(S) \\ f(0) \end{bmatrix} \sim \mathrm{GP}\left[\begin{pmatrix} \mu(S) \\ \mu(0) \end{pmatrix}, \begin{pmatrix} \Sigma(S,S') & \Sigma(S,0) \\ \Sigma(S,0)^T & \Sigma(0,0') \end{pmatrix}\right]. \tag{A2}$$

$\Sigma(S,S')$ is a covariance function for $f(S)$, which is given by $\Sigma(S,S') = \tau^2 \exp[-\phi/\max(S)|S - S'|^2]$. $\Sigma(S,0)$ is a covariance between $f(S)$ and $f(0)$, which is $\Sigma(x,0) = \tau^2 \exp[-\phi/\max(S)|S|^2]$. $\Sigma(0,0')$ is a variance for an univariate Gaussian process prior $f(0)$, which is $\Sigma(0,0') = \tau^2$. With Eqs A1 and A2, we can derive the conditional GP prior:

$$f(S)|f(0) = \ln\alpha \sim \mathrm{GP}[\mu_c, \Sigma_c] \tag{A3}$$

where

$$\mu_c = \mu(S) + \Sigma(S,0)[(0,0')]^{-1}[\ln\alpha - \mu(0)] = \mu(S) \tag{A4}$$

$$\Sigma_c = \Sigma(S,S') - \Sigma(S,0')[\Sigma(0,0')]^{-1}\Sigma(S,0')^T \tag{A5}$$

$$= \tau^2 \exp\left[-\phi\left|\frac{S - S'}{\max(S)}\right|^2\right] - \tau^2 \exp\left\{-\phi\left[\frac{S^2 + S'^2}{\max(S)^2}\right]\right\}.$$

Appendix B: Prior specification and parameter estimation (chapter 3)

B-1. Prior specification

In order for prior distributions to play a minimal role in posterior inference, we want prior distributions for $\ln\alpha, \beta, \phi, \tau^2, \sigma^2$ to be as uninformative as possible. In an extreme case where $\tau^2 \to 0$, fitting the GP prior is equivalent to fitting the Ricker model. Therefore, we used uninformative reference priors developed for the Ricker model (Millar 2002); for the location parameters $\Pr(\ln\alpha, \beta) \propto 1$ and for the scale parameter $\Pr(\sigma^2) \propto \sigma^{-2}$.

However, priors for ϕ and τ^2 had to be specified informatively because our preliminary results showed that the posterior distributions did not converge when uninformative priors were used. Since ϕ controls the number of inflection points in realizations of $f(A)$ (section 3-2-2), the prior for ϕ was determined in light of available biologically plausible models for density dependence, including Allee effects models. These models are usually simple smooth functions with at most 1 inflection point over A. We allowed $f(A)$ to have, on average, 2 inflection points over the range, 0 to $\max(A)$, to capture somewhat more complex shapes. We determined the relationship between ϕ and the expected number of inflection points in $f(A)$ by simulation. We generated $f(A)$ in $A/\max(A) \in [0,1]$ from the GP prior in Eq 4 and counted the number of inflection points in $A\exp[f(A)]$. We found that $\phi = 8$ generates 2 inflection points on average over A. With this information, we used an informative gamma prior distribution with the mean $\mathrm{E}(\phi) = 8$, which is given by $\Pr(\phi) \propto \phi\exp(-\phi/4)$. Note that this prior can be easily overwhelmed by data which clearly show different number of inflection points over A.

For τ^2, we note that the total variance in y is $\mathrm{V}(y) = \mathrm{V}[f(A)] + \sigma^2$, and obtain a ballpark for the variance in y from its observed range (i.e., $r_y = \max(y) - \min(y)$). Assigning the prior variance in y to uncertainty in $f(A)$, we used a gamma prior, $\Pr(\tau^2) \propto \tau^2\exp\left(2\tau^2/r_y\right)$

which has $\mathrm{E}(\tau^2) = r_y$. We conducted prior sensitivity analysis using different parameterization of the gamma prior to determine possibility that the inference of the presence of Allee effects, π, is an artifact of prior specification, and confirmed that π does not change qualitatively across different priors.

B-2. Parameter estimation

With n years of data for data, $(\boldsymbol{A},\boldsymbol{J}) = (\{A_1,\dots,A_n\},\{J_1,\dots,J_n\})$, we have $\boldsymbol{y} = \{\ln(J_1/A_1),\dots,\ln(J_n/A_n)\}$. With data, $f(\boldsymbol{A})$ is a sample from an n dimensional multivariate normal distribution:

$$f(\boldsymbol{A})|\ln\alpha,\beta,\phi,\tau^2 \sim \mathrm{MVN}\left[\mu(\boldsymbol{A}),\Sigma_{f,f}(\boldsymbol{A},\boldsymbol{A'})\right] \tag{B1}$$

where $\mu(\boldsymbol{A}) = ln\alpha\mathbf{1_n} + \beta\boldsymbol{A}/\max(\boldsymbol{A})$ and $\mathbf{1_n}$ is an $n \times 1$ vector of 1's. The i,j^{th} element in the covariance is given by $\Sigma_{f,f}(\boldsymbol{A},\boldsymbol{A'})_{i,j} = \tau^2\exp\left[-\phi|\left(A_i - A_j{}'\right)/\max(\boldsymbol{A})|^2\right]$. Obtaining posterior inference for parameters in this model is computationally cumbersome, but marginalizing over $f(\boldsymbol{A})$ can speed up the computation (Munch et al. 2005):

$$\boldsymbol{y}|\boldsymbol{A},\boldsymbol{\Theta} \sim \mathrm{MVN}\left[\mu(\boldsymbol{A}),\Sigma_{f,f}(\boldsymbol{A},\boldsymbol{A'}) + \sigma^2\boldsymbol{I_n}\right] \tag{B2}$$

$$\boldsymbol{\Theta} \sim Pr(\boldsymbol{\Theta}).$$

$\boldsymbol{I_n}$ is $n \times n$ identity matrix. Parameters in the model are collected in the vector $\boldsymbol{\theta} = \{\ln\alpha,\beta,\phi,\tau^2,\sigma^{-2}\}$ and $\Pr(\boldsymbol{\Theta}) \propto 1 \cdot \phi\exp(-\phi/4) \cdot \tau^2\exp\left(2\tau^2/r_y\right) \cdot \sigma^{-2}$. In light of this, the SB model is essentially identical to an n dimensional multivariate normal likelihood.

We used Metropolis sampling to obtain posterior distributions for τ^2,ϕ,σ^2, at log scale, and Gibbs sampling for $\ln\alpha,\beta$. The assessment for convergence in the updated posterior distributions was conducted using multiple over-dispersed chains (Gelman et al. 2003).

Obtaining inference for an unknown function $f(A)$ was deferred until the posterior distributions for $\boldsymbol{\theta}$ were updated. It follows simply from the fact that the inference for $f(A)$ is sampled from a posterior predictive GP specified with the posterior mean function and the posterior covariance function (see Appendix D) (Munch et al. 2005).

Appendix C: The derivative of a GP, $f'(A)$ (chapter 3)

Given a GP, i.e., $f(A)\sim\mathrm{GP}\left[\mu(A),\Sigma_{f,f}(A,A')\right]$, its derivative, $f'(A)$, is also a GP with mean function $\mu'(A)$ and the covariance function $\Sigma_{f',f'}(A,A')$. Specifically,

$$\frac{df}{dA}\equiv f'(A)\sim\mathrm{GP}\left[\mu'(A),\Sigma_{f',f'}(A,A')\right]. \tag{C1}$$

where $\mu'(A)$ is given by

$$\mu'(A)=\mathrm{E}[\partial f(A)/\partial A]=(\partial\ /\partial A)\mathrm{E}[f(A)]=\beta/\max(A). \tag{C2}$$

And $\Sigma_{f',f'}(A,A')$ is given by

$$\begin{aligned}\Sigma_{f',f'}(A,A') &= \mathrm{E}\left[\frac{\partial f(A)}{\partial A}-\frac{\partial\mu(A)}{\partial A}\right]\left[\frac{\partial f(A')}{\partial A'}-\frac{\partial\mu(A)}{\partial A'}\right]^T \\ &= \frac{\partial}{\partial A}\mathrm{E}[f(A)-\mu(A)][f(A')-\mu(A)]^T\frac{\partial}{\partial A'}^T \\ &= \frac{\partial^2}{\partial A\partial A'}\Sigma_{f,f}(A,A') \\ &= 2\phi\tau^2\left[1-2\phi\left|\frac{A-A'}{\max(A)}\right|^2\right]\exp\left(-\phi\left|\frac{A-A'}{\max(A)}\right|^2\right).\end{aligned} \tag{C3}$$

Similarly, we can determine the covariance between $f(A)$ and $f'(A)$, i.e.,

$$\begin{aligned}\Sigma_{f,f'}(A,A') &= \mathrm{E}\left\{[f(A)-\mu(A)]\left[\frac{\partial f(A')}{\partial A}-\frac{\partial\mu(A')}{\partial A'}\right]^T\right\} \\ &= \mathrm{E}\left\{[f(A)-\mu(A)][f(A')-\mu(A')]^T\right\}\left(\frac{\partial}{\partial A'}\right)^T \\ &= \frac{\partial}{\partial A'}\Sigma_{f,f}(A,A') \\ &= 2\phi\tau^2\left[\frac{A-A'}{\max(A)}\right]\exp\left[-\phi\left|\frac{A-A'}{\max(A)}\right|^2\right].\end{aligned} \tag{C4}$$

Putting these together, the joint distribution for $f(A)$ and $f'(A)$ at a specific point A is the bivariate normal distribution given by:

$$\begin{pmatrix} f(A) \\ f'(A) \end{pmatrix} \sim \mathrm{N}\left[\begin{pmatrix} \ln\alpha + \beta A/\max(A) \\ \beta/\max(A) \end{pmatrix}, \begin{pmatrix} \Sigma_{f,f}(A,A) & \Sigma_{f,f'}(A,A) \\ \Sigma_{f,f}(A,A)^T & \Sigma_{f',f'}(A,A) \end{pmatrix}\right]. \tag{C5}$$

where $\Sigma_{f,f}(A,A)$ is the variance in the GP evaluated at A, $\Sigma_{f',f'}(A,A)$ is the variance of $f'(A)$ at A, and $\Sigma_{f,f'}(A,A)$ is the covariance between $f(A)$ and $f'(A)$ evaluated at A. Plugging $A = A'$ into Eqs C2-4, these are given by:

$$\Sigma_{f,f}(A,A) = \tau^2 \tag{C6}$$

$$\Sigma_{f,f'}(A,A) = 0 \tag{C7}$$

$$\Sigma_{f',f'}(A,A) = 2\phi\tau^2. \tag{C8}$$

Since Allee effects are only relevant for small adult biomass, we used the probability of the presence of Allee effects evaluated at the zero adult biomass, $\Pr[f(0) \leq 0, f'(0) > 0]$, to assess for the presence of Allee effects. To obtain this probability, we marginalized the bivariate normal distribution, $f(0), f'(0)|\boldsymbol{\theta}$ over $\boldsymbol{\theta}$, and integrated numerically:

$$\pi \cong \frac{1}{N}\sum_{i=1}^{N} \iint_{f\in[-\infty,0\},f'\in\{0,\infty]} \Pr[f(0) \leq 0, f'(0) > 0|\boldsymbol{\theta_i}]df df'. \tag{C9}$$

Because the prior distribution for $\ln\alpha$ and β are improper, π prior to incorporating data is also improper. However, because expectation of the joint probability $f(0), f'(0)$ given $\ln\alpha_i, \beta_i, \phi_i, \tau_i^2$ is $[\ln\alpha_i, \beta_i]^T$ and the covariance is 0, this joint distribution is symmetric. Therefore, since we are effectively looking at the probability of being in the upper left quadrant, π prior to incorporating data is 0.25.

Appendix D: Allee effects detection (chapter 3)

The joint multivariate normal distribution for $f(A)$, $f'(A)$, $\boldsymbol{y}$ given the j th set of posterior distributions for the parameter $\boldsymbol{\Theta}$ ($\boldsymbol{\Theta} = \{\ln\alpha, \beta, \phi, \tau^2, \sigma^2\}$) is given by:

$$\begin{pmatrix} f(A) \\ f'(A) \\ \boldsymbol{y} \end{pmatrix} \Bigg| \boldsymbol{A}, \boldsymbol{\Theta} \sim \mathrm{N}\left[\begin{pmatrix} \mu(A) \\ \mu'(A) \\ \mu(\boldsymbol{A}) \end{pmatrix}, \right. \tag{D1}$$

$$\left. \begin{pmatrix} \Sigma_{f,f}(A,A') & \Sigma_{f,f'}(A,A') & \Sigma_{f,f}(A,\boldsymbol{A}') \\ \Sigma_{f,f'}(A,A')^T & \Sigma_{f',f'}(A,A') & \Sigma_{f',f}(A,\boldsymbol{A}') \\ \Sigma_{f,f}(A,\boldsymbol{A}')^T & \Sigma_{f',f}(A,\boldsymbol{A}')^T & \Sigma_{f,f}(\boldsymbol{A},\boldsymbol{A}') + \sigma^2 I_T \end{pmatrix} \right]$$

where $\mu(A) = \ln\alpha + \beta A/\max(A)$, $\mu'(A) = \beta/\max(A)$, and $\mu(\boldsymbol{A}) = \ln\alpha + \beta\boldsymbol{A}/\max(A)$. $\Sigma_{f,f}(A,A')$, $\Sigma_{f,f'}(A,A')$, and $\Sigma_{f',f'}(A,A')$ are given in Appendix B (Eq B1) and C (Eqs C3-4). $\Sigma_{f,f}(A,\boldsymbol{A}')$ is the covariance between the GP evaluated at A and data, $\Sigma_{f',f}(A,\boldsymbol{A}')$ is the covariance between the derivative of the GP evaluated at A and the data, and $\Sigma_{f,f}(\boldsymbol{A},\boldsymbol{A}')$ is the covariance for data. They are given by:

$$\Sigma_{f,f}(A,\boldsymbol{A}') = \tau^2 \exp\left[-\phi\left|\frac{A-\boldsymbol{A}}{\max(\boldsymbol{A})}\right|^2\right] \tag{D2}$$

$$\begin{aligned} \Sigma_{f',f}(A,\boldsymbol{A}') &= \mathrm{E}[\partial f(A)/\partial A - \partial\mu(A)/\partial A][\partial f(A)/\partial A - \partial\mu(A)/\partial A]^T \\ &= (\partial/\partial A)\mathrm{E}[f(A)-\mu(A)][f(A)-\mu(A)]^T \\ &= -2\phi\tau^2\left[\frac{A-\boldsymbol{A}'}{\max(\boldsymbol{A})}\right]\exp\left[-\phi\left|\frac{A-\boldsymbol{A}'}{\max(\boldsymbol{A})}\right|^2\right] \end{aligned} \tag{D3}$$

$$\Sigma_{f,f}(\boldsymbol{A},\boldsymbol{A}') = \tau^2 \exp\left[-\phi\left|\frac{\boldsymbol{A}-\boldsymbol{A}'}{\max(\boldsymbol{A})}\right|^2\right]. \tag{D4}$$

The conditional distribution can be derived by applying a theorem for a standard multivariate normal distribution (e.g., Hogg et al. 2004):

$$f(A), f'(A)|\boldsymbol{A}, \boldsymbol{y}, \boldsymbol{\Theta} \sim \mathrm{N}\left[\psi_{\mathrm{post}}(A), \Omega_{\mathrm{post}}(A, A')\right], \tag{D5}$$

where the posterior mean function $\psi_{\mathrm{post}}(A)$ and the posterior covariance function $\Omega_{\mathrm{post}}(A, A')$ are given by:

$$\begin{aligned}\psi_{\mathrm{post}}(A) = &\begin{bmatrix}\ln\alpha + \beta A/\max(\boldsymbol{A}) \\ \beta/\max(\boldsymbol{A})\end{bmatrix} \\ &+ \begin{bmatrix}\Sigma_{f,f}(A, \boldsymbol{A}') \\ \Sigma_{f',f}(A, \boldsymbol{A}')\end{bmatrix}\left[\Sigma_{f,f}(\boldsymbol{A}, \boldsymbol{A}') + \sigma^2 I_T\right]^{-1}\{\boldsymbol{y} \\ &- [\ln\alpha + \beta\boldsymbol{A}/\max(\boldsymbol{A})]\}\end{aligned} \tag{D6}$$

$$\begin{aligned}\Omega_{\mathrm{post}}(A, A') = &\begin{bmatrix}\Sigma_{f,f}(A, A') & \Sigma_{f,f'}(A, A') \\ \Sigma_{f,f'}(A, A')^T & \Sigma_{f',f'}(A, A')\end{bmatrix} \\ &- \begin{bmatrix}\Sigma_{f,f}(A, \boldsymbol{A}') \\ \Sigma_{f',f}(A, \boldsymbol{A}')\end{bmatrix}\left[\Sigma_{f,f}(\boldsymbol{A}, \boldsymbol{A}') + \sigma^2 I_T\right]^{-1}\begin{bmatrix}\Sigma_{f,f}(A, \boldsymbol{A}') \\ \Sigma_{f',f}(A, \boldsymbol{A}')\end{bmatrix}^T.\end{aligned} \tag{D7}$$

As written in section 3-2-3, we are interested in the posterior inference of Allee effects that are exclusively conditioned on data, $(\boldsymbol{A}, \boldsymbol{J})$, and not dependent specific choice of $\boldsymbol{\Theta}$. We obtained this probabilities, $\Pr[f(A) < 0, f'(A) > 0|\mathrm{data}]$, by Monte Carlo integration over posteriors for $\boldsymbol{\Theta}$. To do so, we first consider a joint posterior distribution for $f(A), f'(A), \boldsymbol{\Theta}$ given data, which can also be written using a rule of a conditional distribution:

$$\Pr[f(A), f'(A), \boldsymbol{\Theta}|\mathrm{data}] = \Pr[f(A), f'(A)|\boldsymbol{\Theta}, \mathrm{data}]\Pr(\boldsymbol{\Theta}|\mathrm{data}), \tag{D8}$$

where $\Pr[f(A), f'(A)|\boldsymbol{\Theta}, \mathrm{data}]$ appeared in Eq D5. We first obtained $\Pr[f(A) < 0, f'(A) > 0|\boldsymbol{\Theta}, \mathrm{data}]$ with numerical integration. Then, using N=1000 random samples of $\boldsymbol{\Theta}$ from the posterior distributions for $\boldsymbol{\Theta}$, $\Pr(\boldsymbol{\Theta}|\mathrm{data})$, we marginalized this distribution over $\boldsymbol{\Theta}$ to obtain $\Pr[f(A) < 0, f'(A) > 0|\mathrm{data}]$. We evaluated this probability for the entire range of $A \in [0, \max(\boldsymbol{A})]$ to generate Figs 2 and 5. We used this posterior probability evaluated at the zero adult biomass, $\pi = \Pr[f(0) \leq 0, f'(0) > 0|\mathrm{data}]$, as an index for detecting Allee effects.

Appendix E: Supplementary results (chapter 5)

Table E1. The summary of parametric (LRT_{Ricker} and LRT_{BH}) and SB analyses (π) of 264 populations' data. N is number of populations of a species. Number in cells for LRT_{Ricker}, LRT_{BH}, and π, indicates number of populations that exhibit evidence for the presence of Allee effects.

Order	Family	*Genus, species* (common name)	N	LRT(R)	LRT(BH)	π
Aulopiformes	Synodontidae	*Harpodon nehereus* (Bombay duck)	1	0	0	0
Clupeiformes	Clupeidae	*Alosa aestivalis* (Blueback herring)	3	0	0	0
		Alosa pseudoharengus (Anadromous alewife)	5	0	0	0
		Alosa sapidissima (Anadromous american shad)	1	0	0	0
		Brevoortia patronus (Gulf Menhaden)	1	0	0	0
		Brevoortia tyrannus (Atlantic Menhaden)	1	0	0	0
		Clupea harengus (Herring)	16	1	2	2
		Sardina pilchardus (Spanish sardine)	1	0	0	0
		Sardinops sagax (Sardine)	2	0	0	0
		Sprattus sprattus (Sprat)	3	0	0	0
	Engraulidae	*Coilia dussumieri* (Gold-spotted grenadier anchovy)	1	0	0	0
		Engraulis encrasicolus (Anchovy)	2	0	0	0
		Engraulis mordax (Northern anchovy)	1	0	0	0
Gadiformes	Gadidae	*Gadus morhua* (Cod)	24	1	0	1
		Melanogrammus aeglefinus (Haddock)	11	0	0	0
		Merlangius merlangus (Black Sea whiting)	2	0	0	0
		Merlangius merlangus (Whiting)	6	0	0	1
		Merluccius bilinearis (Silver hake)	2	0	0	0
		Merluccius capensis (S.A. Hake)	1	0	0	0
		Merluccius merluccius (Hake)	2	0	0	0
		Merluccius productus (Pacific hake)	1	0	0	0
		Micromesistius poutassou (Blue whiting)	1	0	0	0
		Pollachius virens (Pollock or saithe)	5	0	0	0
		Theragra chalcogramma (Walleye pollock)	2	0	0	0
Perciformes	Carangidae	*Trachurus mediterraneus* (Mediterranean horse mackerel)	1	0	0	0
		Trachurus trachurus (Horse mackerel)	1	0	0	0
	Centrarchidae	*Promoxis annularis and nigromaculatus* (Crappie)	4	0	0	0
	Percichthyidae	*Morone saxatilis* (Striped bass)	2	0	0	0
	Percidae	*Stizostedion vitreum* (Walleye)	2	0	0	0
	Pomatomidae	*Pomatomus saltatrix* (Bluefish)	1	0	0	1
	Sciaenidae	*Cynoscion guatucupa* (Weakfish)	1	0	0	0
	Scombridae	*Scomber japonicus* (Chub mackerel)	1	0	0	0
		Scomber scombrus (Mackerel)	2	0	0	0
		Thunnus albacares (Yellowfin tuna)	1	0	0	0
		Thunnus maccoyii (Southern bluefin tuna)	1	0	0	0
		Thunnus obesus (Bigeye Tuna)	3	0	0	1
		Thunnus thynnus (Atlantic bluefin tuna)	1	0	0	0
	Sparidae	*Pagrus pagrus* (Red porgy)	1	0	0	1
	Xiphiidae	*Xiphias gladius* (Swordfish)	1	0	0	0
Pleuronectiformes	Pleuronectidae	*Pleuronectes ferrugineus* (Yellowtail flounder)	2	0	0	0
		Pleuronectes platessa (Plaice)	6	0	0	0
		Reinhardtius hippoglossoides (Greenland halibut)	3	0	0	0
	Soleidae	*Solea vulgaris* (Sole)	5	0	0	0
Scorpaeniformes	Anoplopomatidae	*Anoplopoma fimbria* (Sablefish)	2	0	0	1
	Hexagrammidae	*Pleurogrammus monopterygius* (Atka mackerel)	1	0	0	0
	Scorpaenidae	*Sebastes alutus* (Pacific ocean perch)	4	0	0	0
		Sebastes goodei (Chilipepper rockfish)	1	0	0	0
		Sebastes sp. (Redfish)	1	0	0	0
Salmoniformes	Esocidae	*Esox lucius* (Pike)	2	0	0	0
	Plecoglossidae	*Plecoglossus altivelis* (Ayu)	1	0	0	0
	Salmonidae	*Salmo salar* (Atlantic salmon)	3	0	0	0
		Oncorhynchus gorbuscha (Pink salmon)	51	1	1	1
		Oncorhynchus keta (Chum salmon)	7	0	0	0
		Oncorhynchus nerka (Sockeye salmon)	49	0	1	0
		Oncorhynchus tshawytscha (Chinook salmon)	7	0	0	0
		Salvelinus namaycush (Lake trout)	1	0	0	0
Total			264	3	4	9

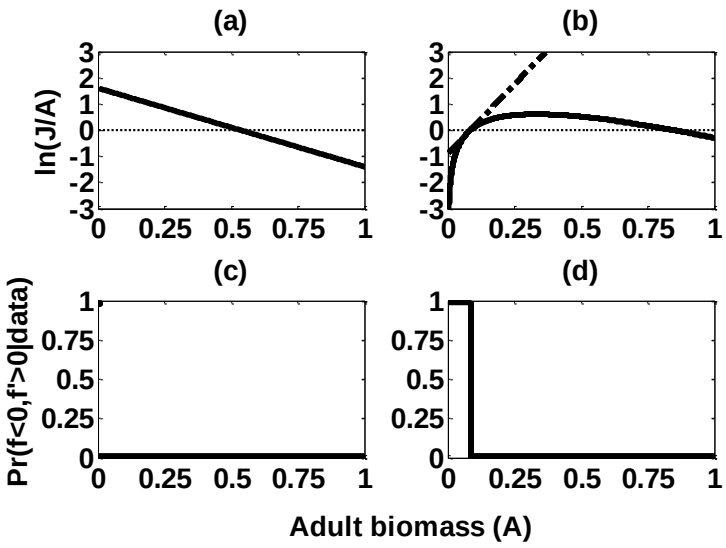

Figure E1. (a) An example of none Allee effects function [solid line]. (b) An example of an Allee effects function [solid line], the derivative of Allee effects function at some A [dot], and the linear approximation of the example Allee effects function at A [broken line]. (c) The probability for the presence of Allee effects, $\Pr[f(A)\leq 0, f'(A)>0|\text{data}]$, obtained from the example function used in (a). (d) The probability for the presence of Allee effects obtained from the example function used in (b).

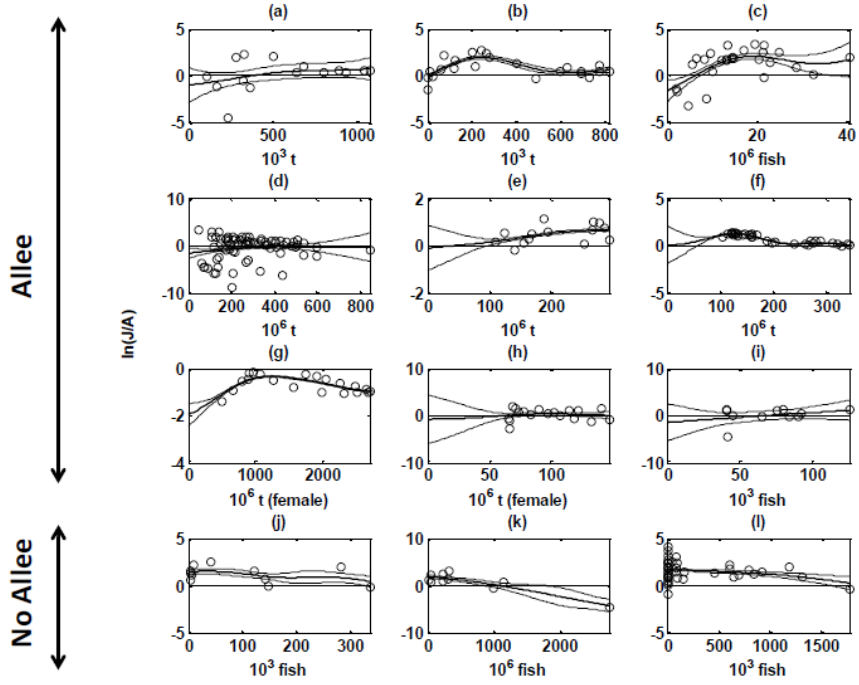

Figure E2. The posterior inference of $f(A)$ for 12 population datasets which exhibit Allee effects. 'Allee' indicates populations which the SB model detected Allee effects (a-i). 'No Allee' indicates populations which only parametric models detected Allee effects (j-l). We plotted data [dots], the mean of the posterior $f(A)$ [thick solid line], and the 95% confidence intervals of the posterior $f(A)$ [thin solid line]. Note that scales in x and y axis differ across different populations. (a) Atlantic herring (Georges bank), (b) Atlantic herring (Iceland spring spawner), (c) Atlantic cod (The Newfound land, Canada), (d) whiting (North Sea), (e) bluefish (East Coast, USA), (f) bigeye tuna (West Atlantic), (g) red porgy (Atlantic ocean off North Carolina), (h) sablefish (West Coast, USA), (i) pink salmon (Burke, B.C., Canada), (j) pink salmon (Kitimat, B.C., Canada), (k) pink salmon (Utka river, Kamchatka, Russia), (l) sockeye salmon (Adams Complex, B.C., Canada).